

Theory of Anderson transition in three-dimensional chiral symmetry classes: Connection to type-II superconductors

Pengwei Zhao and Ryuichi Shindou*

International Center for Quantum Materials, Peking University, Beijing 100871, China

(Dated: June 27, 2025)

Phase transitions governed by topological defects constitute a cornerstone of modern physics. Two-dimensional (2D) Anderson transitions in chiral symmetry classes are driven by the proliferation of vortex-antivortex pairs—a mechanism analogous to the Berezinskii–Kosterlitz–Thouless (BKT) transition in the 2D XY model. In this work, we extend this paradigm to three-dimensional (3D) chiral symmetry classes, where vortex loops emerge as the key topological defects governing the Anderson transition. By deriving the dual representation of the 3D nonlinear sigma model for the chiral unitary class, we develop a mean-field theory of its Anderson transition and elucidate the role of 1D weak band topology in the Anderson transition. Strikingly, our dual representation of the 3D NLSM in the chiral symmetry class uncovers its connection to the magnetostatics of 3D type-II superconductors. The metal-to-quasi-localized and quasi-localized-to-insulating transitions in 3D chiral symmetry class share a unified theoretical framework with the normal-to-mixed and mixed-to-superconducting transitions in 3D type-II superconductors under an external magnetic field, respectively.

I. INTRODUCTION

Topological defects are universal entities in physical systems with symmetries [1, 2]. Characterized by quantized charges, topological defects exhibit remarkable stability against local perturbations. Well-known examples include domain walls in Ising magnets [3, 4], vortices in superconductors and superfluids [5–9], and skyrmions in Heisenberg magnets [10–14]. Thermodynamic properties of physical systems are profoundly influenced by topological defects, whose spatial proliferation introduces disorder in an ordered phase, leading to dramatic changes in the macroscopic properties of the systems. This mechanism drives fundamental phase transitions, such as Berezinskii–Kosterlitz–Thouless (BKT) transition [15–18], melting transitions of 2D solids [19–21], and the superfluid transition [5, 6, 22–25], underscoring the pivotal role of topological defects in shaping collective phenomena [26–28].

In disordered electron systems—such as an electron gas with random impurities—charge carriers experience repeated scattering events that reduce their mean-free time. In the weak disorder regime, electrons retain sufficient coherence to propagate diffusively, resulting in a metallic phase with finite conductivity. When disorder strength exceeds a critical disorder strength, the random potentials cause spatial localization of electronic states [29–31]. This metal-insulator transition, known as the Anderson transition, has been experimentally studied in diverse wave systems, which include not only electron waves in solid-state materials [32, 33] but also electromagnetic and atomic waves in optical, photonic, and cold-atom systems [34–37].

Decades of theoretical and numerical studies [38–49] have demonstrated that the Anderson transitions exhibit

universal scaling behaviors characterized by critical exponents, which define distinct universality classes. The universality classes are classified according to fundamental Hamiltonian symmetries—time-reversal (TRS), particle-hole (PHS), and chiral (CS) symmetries—which constitute the celebrated Altland–Zirnbauer ten-fold way [46]. The classification scheme has since been extended to non-Hermitian matrices [50–52] and their eigenstates’ localization phenomena [53–55], revealing its broad applicability in the study of non-Hermitian disordered systems [54, 56–78].

Despite decades of research, the nature of the Anderson transition in some symmetry classes remains enigmatic [79–104]. The Anderson transition has been studied by using effective field theories for disordered quantum systems—nonlinear sigma models (NLSMs)—in which the coupling constant corresponds to conductivity, and the β function of the conductivity determines the presence (or absence) of the Anderson transition as well as its universality class [38–43, 48]. In the early 90s, Gade and Wegner found that the perturbative β function for chiral symmetry classes (AIII, CII, and BDI) has no localization effects in the dimension $D \geq 2$, implying that metallic phases in these classes remain stable regardless of disorder strength—contrary to the expectation that sufficiently strong disorder should always induce the Anderson transition [79, 80]. The puzzle was later resolved in 2D by König et al. [95], who incorporated non-perturbative effects arising from topological defects in the NLSMs. The NLSM field variable in chiral symmetry classes resides in curved manifolds of the unitary group. Such manifolds inherently possess a $U(1)$ subgroup symmetry, permitting vortex solutions. Thus, the 2D Anderson transition in chiral symmetry classes can be understood as a quantum phase transition driven by the spatial proliferation of $U(1)$ vortex-antivortex pairs [95, 103]. In contrast, the theoretical framework of the 3D Anderson transition in chiral symmetry classes remains largely unexplored, despite nu-

* rshindou@pku.edu.cn

merical confirmations of its existence [92, 97, 99, 102].

In this paper, we generalize the 2D theory [95] into three-dimensional (3D) chiral symmetry classes, where the NLSM field variable permits vortex *loop* solutions. We argue that the 3D Anderson transition in chiral classes is driven by the spatial proliferation of the vortex loops. We derive a dual representation of the 3D NLSM for the chiral unitary class and construct a mean-field theory of its 3D Anderson transition. The dual model takes the form of $U(N)$ type-II superconductors.

- The diffusive metal phase with a sparse population of vortex loops is described as the normal (Maxwell) phase in the type-II superconductors, where magnetic gauge field fluctuations—driven by the entropic effect but controlled by the Maxwell action—suppress superconductivity entirely.
- The localized phase, signaled by vortex-loop proliferation, is described as the superconducting (Meissner) phase, where the Josephson coupling stabilizes superconducting order, and the spontaneous symmetry breaking of the global $U(1)$ gauge symmetry renders the magnetic gauge field massive via the Anderson-Higgs mechanism [105, 106].

Recent studies have demonstrated that nontrivial 1D weak band topology in chiral symmetry classes gives rise to an intermediate quasi-localized phase, bridging metallic and fully localized phases [102, 103]. In the quasi-localized phase, the exponential localization length diverges only along the weak topological direction while remaining finite in the other directions. We show that, in the dual representation, the 1D weak topology manifests as an external magnetic field applied to the type-II superconductors along the topological direction. Thereby,

- the quasi-localized phase—characterized by divergent localization length only along the topological direction—can be described as an intermediate mixed phase in which the external magnetic field penetrates through the 3D superconducting bulk in the form of magnetic flux tubes [107–109].

The remainder of this paper is organized as follows. Section II introduces the NLSM for chiral symmetry classes. In Appendix A, we outline a derivation of the NLSM for the chiral unitary class. Section III and Appendix B explain the topological defects in the 3D NLSM in the chiral symmetry classes and their qualitative impact on the localization properties of chiral symmetry classes. Section IV develops the dual representation of the NLSM. Section V and Appendix C analyze the dual lattice model without the 1D weak topology. Section VI analyzes the dual lattice model with the 1D weak topology and discusses the nature of the quasi-localized phase. Section VII summarizes the paper.

II. NONLINEAR SIGMA MODEL

A disordered system considered here consists of a free-fermion Hamiltonian perturbed by a single-particle random potential, where the random potential follows a certain probability distribution. Physical observables in such systems are determined through two distinct averaging procedures. One is the quantum-mechanical average $\partial \ln \mathcal{Z} / \partial J$, where \mathcal{Z} is a partition function of the free-particle Hamiltonian with some potential, and J is a current operator that couples linearly with the observables. The other is a subsequent disorder average, $\langle \ln \mathcal{Z} \rangle_{\text{dis}}$, over the potential's probability distribution. To evaluate $\langle \ln \mathcal{Z} \rangle_{\text{dis}}$, three formalisms are commonly employed: replica formulation (used here) [38–40, 110], supersymmetry technique [43, 111], and Keldysh path integral formalism [112]. The replica formulation exploits the mathematical identity:

$$\ln \mathcal{Z} = \lim_{N \rightarrow 0} \frac{\mathcal{Z}^N - 1}{N}. \quad (1)$$

For a Gaussian-distributed random potential, the disorder average of the replicated partition function $\langle \mathcal{Z}^N \rangle_{\text{dis}}$ can be computed exactly. Upon integrating the disorder potential over the Gaussian distribution function, the system acquires an effective interaction among N replicated free-fermion fields. This interaction is then decoupled by the use of a Hubbard-Stratonovich matrix field (Q field), leading to a self-consistent Born equation for the fermion mean free time τ .

In the weak disorder regime, the fermion has a finite mean-free time τ , which spontaneously breaks continuous symmetries in a space of the N replicated fields [38–40, 83]. Low-energy thermodynamics in the weak disorder regime is governed by gapless Goldstone (diffusion) modes arising from the continuous symmetry breaking, and it can be studied in terms of the spatial gradient expansion of the slowly-varying Q -field. Up to the second-order gradient expansion, an effective action for the Goldstone modes in chiral symmetry classes is described by the following NLSM [79, 80, 83–85, 95, 103]:

$$S = - \int \frac{d^3 r}{8\pi s} \sum_{\mu=x,y,z} \left[\sigma_\mu \text{Tr} (Q^{-1} \nabla_\mu Q)^2 + c_\mu \text{Tr}^2(Q^{-1} \nabla_\mu Q) - \chi_\mu \text{Tr} (Q^{-1} \nabla_\mu Q) \right], \quad (2)$$

with the disorder-averaged replicated partition function $Z \equiv \langle \mathcal{Z}^N \rangle_{\text{dis}} = \int D[Q] e^{-S}$ (see also Appendix A). The Q -field resides on a curved manifold dubbed the Goldstone manifold, and $D[Q]$ is a Haar measure on the curved manifold [113]. For chiral unitary, symplectic, and orthogonal classes, the Q field is $U(N)$, $U(N)/O(N)$, and $U(N)/\text{Sp}(N)$, respectively [48, 95] (Table I).

In Eq. (2), the first term with conductivity σ_μ governs dynamics of the gapless Goldstone modes—diffusion phenomena. The second term with the so-called Gade

Symmetry class	Goldstone manifold	Extra constraint	s
AIII	$U(N)$	None	1
CII	$U(N)/O(N)$	$Q = Q^T$	2
BDI	$U(N)/Sp(N)$	$Q = CQ^T C$	2

TABLE I. The Goldstone manifold where the field variable Q lives for three chiral symmetry classes. $U(N)$, $O(N)$, and $Sp(N)$ are the unitary, orthogonal, and symplectic groups, respectively. C is a skew-symmetric matrix that satisfies $C^2 = 1$.

constant c_μ arises from couplings between the gapless Goldstone modes and high-energy massive modes. [83–85, 103] A real-valued vector χ represents the 1D weak band topology, which encodes the 1D topological index of an underlying 3D lattice model [103, 114, 115]. In this paper, we refer to a spatial direction along χ as a topological direction. For simplicity, in the following section, we assume spatially isotropic conductivity and Gade constant: $\sigma_\mu = \sigma$, $c_\mu = c$.

III. TOPOLOGICAL DEFECT

A. Saddle-point equation

The Goldstone manifolds in all three chiral symmetry classes have a $U(1)$ subgroup. An eigenvalue of the Q field in such Goldstone manifolds has a vortex excitation as a stable topological defect, which takes the form of a line in 3D space [5, 6]. To describe general forms of vortex excitations in the Q field, consider an eigenvalue $e^{i\phi_n(\mathbf{r})}$ and eigenvector $|p_n(\mathbf{r})\rangle$ of the Q field ($n = 1, \dots, N$), respectively,

$$Q(\mathbf{r}) = \sum_{n=1}^N e^{i\phi_n(\mathbf{r})} |p_n(\mathbf{r})\rangle \langle p_n(\mathbf{r})|. \quad (3)$$

$|p_n(\mathbf{r})\rangle$ in the AIII class has no symmetry constraint, belonging to the complex projective space $\mathbb{C}P^{N-1}$. The eigenvectors in the BDI class form Kramers doublet, $|p_{n,\sigma}(\mathbf{r})\rangle$ ($\sigma = \pm$), for each eigenvalue $e^{i\phi_n(\mathbf{r})}$ ($n = 1, \dots, N/2$), belonging to the quaternionic projective space $\mathbb{H}P^{N/2-1}$. The eigenvectors in the CII class are real-valued, belonging to the real projective space $\mathbb{R}P^{N-1}$ [95]. Being a unit complex number, each eigenvalue $e^{i\phi_n(\mathbf{r})}$ permits a vortex excitation. In 3D space, a vortex excitation forms a closed line C of quantized vortex – vortex loop –

$$\sum_{\nu,\rho} \epsilon_{\mu\nu\rho} \nabla_\nu \nabla_\rho \phi_n(\mathbf{r}) = 2\pi\eta \oint_C dl_\mu \delta^3(\mathbf{r} - \mathbf{l}). \quad (4)$$

Here $\eta \in \mathbb{Z}$ stands for vorticity, and a line integral on the right-hand side is along the vortex loop C . Each eigenvalue has an arbitrary number of vortex loops [103].

The Q field with the vortex excitations can be introduced as a saddle-point solution of the chiral NLSM,

Eq. (2). To this end, consider the following *ansatz* as a saddle-point solution [95, 103], which assumes that all the eigenvalues except for $e^{i\phi(\mathbf{r})}$ are degenerate, and only $e^{i\phi(\mathbf{r})}$ has multiple vortex loops:

$$Q(\mathbf{r}) = 1 + \left[e^{i\phi(\mathbf{r})} - 1 \right] |p(\mathbf{r})\rangle \langle p(\mathbf{r})|. \quad (5)$$

Here $P(\mathbf{r}) \equiv |p(\mathbf{r})\rangle \langle p(\mathbf{r})|$ is a projection operator onto the one-dimensional and two-dimensional eigenspaces of $e^{i\phi(\mathbf{r})}$ in the AIII and CII classes, and the BDI class, respectively. A substitution of the *ansatz* into the NLSM action Eq. (2) yields,

$$S[\phi, P] = \int \frac{d^3r}{8\pi s} [(\sigma + c)(\nabla_\mu \phi)^2 + 2\sigma(1 - \cos \phi) \text{Tr}(\nabla_\mu P)^2 + i\chi_\mu \nabla_\mu \phi]. \quad (6)$$

From $\delta S/\delta \phi(\mathbf{r}) = 0$ and $\delta S/\delta P(\mathbf{r}) = 0$, we obtain saddle-point equations for $\phi(\mathbf{r})$ and $P(\mathbf{r})$, respectively,

$$\sum_\mu (\sigma + c) \nabla_\mu^2 \phi + \sum_\mu \sin \phi \text{Tr}(\nabla_\mu P)^2 = 0, \quad (7)$$

$$\sum_\mu \sigma(1 - \cos \phi) \nabla_\mu^2 P + \sum_\mu \sigma \sin \phi \nabla_\mu \phi \nabla_\mu P = 0. \quad (8)$$

When $\phi(\mathbf{r})$ is definite, such as outside the vortex cores, the second equation requires that $P(\mathbf{r})$ is independent of \mathbf{r} (Appendix B). When $\phi(\mathbf{r})$ is indefinite such as at the vortex cores, $P(\mathbf{r})$ can depend on \mathbf{r} . Thus, the first equation yields the Poisson equation $\nabla^2 \phi = 0$. The Poisson equation supports saddle-point solutions with multiple vortex loops,

$$\sum_{\nu,\rho} \epsilon_{\mu\nu\rho} \nabla_\nu \nabla_\rho \phi(\mathbf{r}) = 2\pi \sum_{j=1}^n \oint_{C_j} dl_\mu \delta^3(\mathbf{r} - \mathbf{l}), \quad (9)$$

where C_j defines the 3D coordinate of the j th vortex loop with the unit vorticity ($\eta_j = 1$). For simplicity, we henceforth consider only vortex loops with the unit vorticity, because a vortex line with higher vorticities can be regarded as a sum of several vortex lines with the unit vorticity. As $P(\mathbf{r})$, except at the vortex cores, is independent of \mathbf{r} , the energy of the saddle-point solution may as well be expressed by a functional only of $\phi(\mathbf{r})$;

$$S[\phi, P] = S[\phi] \equiv \int \frac{d^3r}{8\pi s} \sum_\mu [(\sigma + c) (\nabla_\mu \phi)^2 + i\chi_\mu \nabla_\mu \phi]. \quad (10)$$

We note in passing that the \mathbf{r} -dependence of $P(\mathbf{r})$ along the vortex core may bring additional positive energies from the second term of Eq. (6). For simplicity, in this section, we ignore such $P(\mathbf{r})$ -dependent energy terms [see also Section IV for an alternative way of including the effect of $P(\mathbf{r})$].

B. Vortex-driven Q -field fluctuation and effect of 1D weak topology

The saddle-point equations and their solutions have a physical analogy to 3D magnetostatics in the presence of quantized electric current loops [116]. Regarding ϕ as a magnetic scalar potential and defining $\mathbf{h} \equiv -\nabla\phi$, the Poisson equation becomes the magnetic Gauss law, $\nabla \cdot \mathbf{h} = 0$. Meanwhile, Eq. (9) can be recast as the Biot-Savart law for \mathbf{h} , where a vortex loop becomes a quantized electric current loop.

The analogy to the 3D magnetostatics is useful for discussing the Q -field fluctuation induced by the vortex excitations. The effect of vortex excitations on the Q -field fluctuation may be characterized by a correlation function of the U(1) phase variable, $e^{i\phi(\mathbf{r})}$,

$$F(\mathbf{r} - \mathbf{r}') \equiv \left\langle e^{i[\phi(\mathbf{r}') - \phi(\mathbf{r})]} \right\rangle. \quad (11)$$

Here the average in the right-hand side is over $\phi(\mathbf{r})$ with and without vortex excitations, $\langle \dots \rangle \equiv \frac{1}{Z} \int \mathcal{D}[\phi] \dots \exp(-S[\phi])$, and $Z \equiv \int \mathcal{D}[\phi] \exp(-S[\phi])$. The fluctuation of the ϕ field comprises the spin-wave part ϕ_{sw} and the vortex-excitation part ϕ_{v} . When the spin-wave part is neglected, the phase difference is rewritten by an integral of the magnetic field \mathbf{h} along an arbitrary line connecting \mathbf{r} and \mathbf{r}' ,

$$\begin{aligned} F(\mathbf{r} - \mathbf{r}') &\simeq \left\langle e^{i \int_{\mathbf{r}'}^{\mathbf{r}} d\mathbf{s} \cdot \mathbf{h}(\mathbf{s})} \right\rangle_{\text{v}} \\ &\equiv \frac{1}{Z_{\text{v}}} \int \mathcal{D}[\phi_{\text{v}}] e^{i \int_{\mathbf{r}'}^{\mathbf{r}} d\mathbf{s} \cdot \mathbf{h}(\mathbf{s})} e^{-S_{\text{v}}}, \end{aligned} \quad (12)$$

with $Z_{\text{v}} \equiv \int \mathcal{D}[\phi_{\text{v}}] e^{-S_{\text{v}}}$. Here the action in Eq. (10) is decomposed into the spin wave part $S_{\text{sw}} = \int d^3r / (8\pi) (\sigma + Nc) (\nabla_{\mu} \phi_{\text{sw}})^2$ and vortex excitation part, S_{v} with $S = S_{\text{sw}} + S_{\text{v}}$. From the analogy to the 3D magnetostatics, the vortex part S_{v} of Eq. (10) takes the form of a Coulomb loop gas model, where the vortex loops (electric current loops) interact with each other via the $1/r$ Coulomb interaction [117–122]. The 1D Berry phase term confers the complex phase factor upon each closed vortex loop [103, 122, 123],

$$S_{\text{v}} = g \sum_{j,m} \oint_{C_j} \oint_{C_m} \frac{d\mathbf{r}_j \cdot d\mathbf{r}_m}{|\mathbf{r}_j - \mathbf{r}_m|} + i\bar{\chi}_{\mu} \sum_j \epsilon_{\mu\nu\rho} \Gamma_{j,\nu\rho}. \quad (13)$$

Here $g \equiv (\sigma + c)/(8s)$ and $\bar{\chi} \equiv \chi/(4s)$, $j, m = 1, \dots, n$, $\mu, \nu, \rho = x, y, z$, and $d\mathbf{r}_j$ and $d\mathbf{r}_m$ are tangential vectors of the j th and m th vortex loops C_j and C_m at \mathbf{r}_j and \mathbf{r}_m , respectively. Note that the vortex loop segments (electric-current loop segments) interact via the $1/r$ Coulomb interaction. $\Gamma_{j,\nu\rho}$ is a projected area of the j th vortex loop onto the ν - ρ plane. The path integral $\int \mathcal{D}[\phi_{\text{v}}]$ over the vortex excitation part is nothing but a sum over all possible configurations of vortex loops,

$$\int \mathcal{D}[\phi_{\text{v}}] \equiv 1 + \sum_{n=1}^{\infty} \frac{1}{n!} \prod_{j=1}^n \left(\int dl_j t^j \int d^3R_j \int \mathcal{D}\Omega_j(\lambda) \right). \quad (14)$$

The right-hand side comprises a sum over vortex-loop number n , an integral over a length l_j of the j th vortex loop C_j ($j = 1, \dots, n$), an integral over a center-of-mass coordinate R_j of the j th loop, and a path integral over the tangential vector $\Omega_j(\lambda) \equiv d\mathbf{r}_j(\lambda)/d\lambda$ in the loop C_j (Here λ is a 1D length-scale parameter that parametrizes the loop segment in the loop). With a closed-loop condition of $\int_0^{l_j} d\lambda \Omega_j(\lambda) = 0$, the path integral over the tangential vector is equivalent to a summation over possible shapes of the closed loop with a fixed length l_j [122]. Note that a fugacity parameter t of the vortex loop is newly included on the right-hand side: $\ln t$ is a chemical potential of the vortex loop segment per unit length. $1/n!$ is a symmetry factor that sets off double counting of the same multiple-vortex-loops configurations.

The Coulomb loop gas model without the 1D Berry phase term ($\chi = 0$) undergoes an order-disorder transition driven by the spatial proliferation of vortex loops (electric-current loops). The transition was previously studied by a renormalization group method, which copes with the screening effect of smaller vortex loops upon the Coulomb interaction among larger vortex loops [24, 25, 122]. The screening effect renormalizes the coupling constant g , while a short-range part of the Coulomb interaction renormalizes the fugacity parameter $\ln t$. The RG study shows that the ordered phase is characterized by a fixed point with divergent g and vanishing t , and the disordered phase is characterized by a fixed point with vanishing g and divergent t . In fact, the divergent t results in the spatial proliferation of vortex loops (electric-current loops), which makes the magnetic field $\mathbf{h}(\mathbf{r})$ to be statistically indefinite, rendering the correlation function Eq. (12) to be vanishing for $|\mathbf{r}' - \mathbf{r}| \neq 0$.

The authors previously proposed that the 1D Berry phase term χ universally induces an intermediate quasi-disordered phase between the ordered and disordered phases [103, 122]. In the quasi-disordered phase, an exponential correlation length of the U(1)-phase correlation function is divergent along χ , while it is finite along the other directions. According to the Coulomb loop gas model in Eq. (13), a vortex loop adds to the partition function a complex phase factor, and the phase is proportional to an area within the loop projected onto a plane perpendicular to χ . On the other hand, a polarized vortex loop—a vortex loop that is confined in a plane parallel to χ —does not induce any phase factor. Consequently, the complex phase factor selectively causes destructive interference among configurations of those vortex loops that have finite projections to the plane, and the partition function in the ordered phase can be dominated by the polarized vortex loops, especially near a boundary of the ordered phase. In fact, the renormalization group analysis shows that the 1D Berry phase term suppresses the screening effect of unpolarized vortex loops, while the screening effect of the polarized vortex loops confines the larger vortex loops into planes parallel to χ , as well as stretches them along the χ direction [122]. The proliferation of the polarized vortex loops makes the

U(1)-phase correlation perpendicular to the χ direction [Eq. (12) for $\mathbf{r} - \mathbf{r}' \perp \chi$] to be strongly disordered, while leaving intact the correlation function along the χ directions [Eq. (12) for $\mathbf{r} - \mathbf{r}' \parallel \chi$]. This may result in the emergence of the quasi-disorder phase next to the ordered phase, in which the exponential correlation length of the U(1)-phase correlation function is divergent only along χ . Such an intermediate quasi-disorder phase is consistent with the phenomenology of the quasi-localized phase in the chiral symmetric systems with the 1D weak band topology [102, 103]. To promote this perspective, in the next section, we further elaborate on the analogy to the magnetostatics and derive a dual representation of the 3D chiral NLSM.

IV. DUALITY TRANSFORMATION

In the previous section, we showed that the saddle-point solution of the action is characterized by multiple vortex-loop configurations of an eigenvalue $e^{i\phi(\mathbf{r})}$ of the Q field, and its associated eigenvector $|p(\mathbf{r})\rangle$ at vortex cores. In this section, we start from the partition function in the saddle-point manifold coordinated by these degrees of freedom, and derive its dual representation. Based on the dual model, we will argue in the next section a mean field theory of the Anderson transition and the quasi-localization phenomena in the chiral symmetry class. For simplicity, we focus on the chiral unitary class (class AIII). Note that the duality transformation could be implemented in several different ways, depending on how to take a sum over vortex-loop configurations in the 3D space [119–121, 124]. In this paper, we place the continuous field theory into a 3D cubic lattice and derive a lattice version of the U(N) type-II superconductor model. As in Ref. [125], one may also employ the particle-field duality and derive a U(N) generalization of the Anderson-Higgs model.

A. Dual continuum theory

The partition function in the saddle-point manifold involves the $Q(\mathbf{r})$ -field integral, while the $Q(\mathbf{r})$ field is a U(N) matrix field with the nonlinear constraint $Q^\dagger Q = 1$. To cope with the integral over such a curved manifold, we transform the integral variables into elements of the u(N) Lie algebra via $\mathbf{h} \equiv -iQ^{-1}\nabla Q$: the u(N) field resides in a flat space [95, 103]. In terms of the h field, the action of the chiral NLSM reads

$$S = \int \frac{d^3r}{8\pi} \sum_{\mu=x,y,z} (\sigma \text{Tr} h_\mu^2 + c \text{Tr}^2 h_\mu + i\chi_\mu \text{Tr} h_\mu). \quad (15)$$

The saddle-point manifold is coordinated by configurations of vortex loops and $|p(\mathbf{r})\rangle$ at vortex cores. To relate the \mathbf{h} field with these degrees of freedom, we introduce a field strength vector $F_\mu = \epsilon_{\mu\nu\rho} \nabla_\nu h_\rho + i\epsilon_{\mu\nu\rho} h_\nu h_\rho$ [95, 103].

The field strength vector is directly given by the vortex loop configuration and $|p(\mathbf{r})\rangle$ at vortex cores (see Appendix B),

$$\begin{aligned} F_\rho(\mathbf{r}) &= \epsilon_{\rho\mu\nu} \nabla_\mu \nabla_\nu \phi(\mathbf{r}) |p(\mathbf{r})\rangle \langle p(\mathbf{r})| \\ &= 2\pi \sum_{j=1}^n \oint_{C_j} dl_\rho \delta^3(\mathbf{r} - \mathbf{l}) P(\mathbf{r}) \equiv J_\rho(\mathbf{r}), \end{aligned} \quad (16)$$

with $P(\mathbf{r}) \equiv |p(\mathbf{r})\rangle \langle p(\mathbf{r})|$ and Eq. (4). Thus, by equating the right-hand side with u(N)-valued vortex vector field $J_\rho(\mathbf{r})$ ($\rho = x, y, z$), we can write the partition function in the saddle-point manifold as follows,

$$Z = \int D[\mathbf{h}] \int D[\mathbf{J}] \delta[\mathbf{F} - \mathbf{J}] \exp(-S). \quad (17)$$

Here the integral of \mathbf{h} is over the u(N) elements, while an integral of \mathbf{J} comprises the sum over all possible multiple vortex-loop configurations, and the integral over $|p(\mathbf{r})\rangle$,

$$\int D[\mathbf{J}] \equiv \int D[\phi_v] \int D[P]. \quad (18)$$

$\int D[\phi_v]$ is defined in Eq. (14), and $\int D[P]$ stands for multiple integrals over $|p(\mathbf{r})\rangle$ at every \mathbf{r} along vortex lines;

$$\int D[P] \equiv \prod_{\mathbf{r} \in \{C_j\}} \int d|p(\mathbf{r})\rangle. \quad (19)$$

The constraint $\mathbf{F} = \mathbf{J}$ can be implemented by an integral of a u(N)-valued auxiliary vector field $\Theta_\rho(\mathbf{r})$ ($\rho = x, y, z$)

$$\delta[\mathbf{F} - \mathbf{J}] = \int D[\Theta] \exp \left\{ i \int d^3r \text{Tr} [\Theta \cdot (\mathbf{F} - \mathbf{J})] \right\}. \quad (20)$$

Thanks to the auxiliary field, the partition function becomes integrable over the h field. The integration yields an action only of the auxiliary field $\Theta(\mathbf{r})$ [103],

$$Z = \int D[\Theta] e^{-S_{\text{dual}}}, \quad S_{\text{dual}} = S_{\text{u}(1)} + S_{\text{su}(N)} + S_t, \quad (21)$$

$$S_{\text{u}(1)} = \frac{2\pi}{\sigma + Nc} \int d^3r \left(\nabla \times \theta^0 - \frac{\sqrt{N}}{8\pi} \chi \right)^2, \quad (22)$$

$$S_{\text{su}(N)} = \frac{2\pi}{\sigma} \int d^3r \sum_{a=1}^{N^2-1} (\nabla \times \theta^a)^2 + \mathcal{O}(\sigma^{-2}), \quad (23)$$

$$\begin{aligned} S_t &= - \int dl^t \int d^3R \int D\Omega(\lambda) \int D|p(\mathbf{r}(\lambda))\rangle \\ &\exp \left\{ 2\pi i \oint_C dl_\rho \left[\frac{\theta_\rho^0(\mathbf{l})}{\sqrt{N}} + \sum_{a=1}^{N^2-1} \theta_\rho^a(\mathbf{l}) \langle p(\mathbf{l}) | T^a | p(\mathbf{l}) \rangle \right] \right\}. \end{aligned} \quad (24)$$

Here θ^0 and θ^a ($a = 1, \dots, N^2 - 1$) are real-valued expansion coefficients of the Θ field in terms of the u(1) basis $T^0 \equiv 1/\sqrt{N}$ and su(N) bases T^a , respectively,

$$\Theta_\rho(\mathbf{r}) = \theta_\rho^0(\mathbf{r}) T^0 + \sum_{a=1}^{N^2-1} \theta_\rho^a(\mathbf{r}) T^a, \quad (25)$$

with $\text{Tr}(T^0 T^a) = 0$, and $\text{Tr}(T^a T^b) = \delta_{ab}$.

The dual theory Eq. (21) respects a local U(1) gauge symmetry;

$$\theta^0(\mathbf{r}) \rightarrow \theta^0(\mathbf{r}) + \nabla\varphi(\mathbf{r}), \quad (26)$$

with a rotation-free vector field $\nabla\varphi(\mathbf{r})$. Thus, $\theta^0(\mathbf{r})$, $S_{u(1)}$, and $\sigma + Nc$ can be interpreted as a magnetic gauge field, the magnetic part of the Maxwell action, and magnetic permeability, respectively. Similarly, $S_{su(N)}$ can be also regarded as SU(N) generalization of the Maxwell action, while the dual theory does not have additional gauge symmetries associated with $\theta^a(\mathbf{r})$ ($a = 1, \dots, N$). In $S_{su(N)}$, higher-order terms in $1/\sigma$, which encode interactions among SU(N) gauge fields, are neglected. The approximation may be justified near the metallic phase, where σ is sufficiently large. S_t comprises a sum over all possible configurations of *single* vortex loop, yielding highly nonlocal interactions among the gauge fields.

The duality transformation also connects the correlation function, Eq. (11), to a ratio of the dual theory's partition functions with and without a pair of magnetic charges. As $\partial_\mu\phi = \text{Tr} h_\mu \equiv h_\mu^0 \sqrt{N}$, Eq. (11) can be expressed by a line integral of the u(1) component h_μ^0 ,

$$\begin{aligned} \langle e^{i\phi(\mathbf{r}_1) - i\phi(\mathbf{r}_2)} \rangle &= \frac{1}{Z} \int D[\mathbf{h}] \int D[\mathbf{J}] \delta[\mathbf{F} - \mathbf{J}] \\ &\times \exp \left[-S + i\sqrt{N} \int_{\mathbf{r}_2}^{\mathbf{r}_1} d\mathbf{l} \cdot \mathbf{h}^0(\mathbf{l}) \right] \\ &= \frac{1}{Z} \int D[\Theta] \exp [-S_{u(1)}[v^D(\mathbf{r})] - S_{su(N)} - S_t], \quad (27) \end{aligned}$$

with

$$\begin{aligned} S_{u(1)}[v^D(\mathbf{r})] &= \\ \frac{2\pi}{\sigma + Nc} \int d^3r &\left[\nabla \times \theta^0 - \frac{\sqrt{N}}{8\pi} \chi + \sqrt{N} v^D(\mathbf{r}) \right]^2. \quad (28) \end{aligned}$$

On the right-hand side of Eq. (28), $v^D(\mathbf{r})$ represents a quantized magnetic flux emanating from a magnetic monopole at \mathbf{r}_1 to a magnetic anti-monopole at \mathbf{r}_2 ,

$$v_\mu^D(\mathbf{r}) \equiv \int_{\mathbf{r}_2}^{\mathbf{r}_1} d\mathbf{l}_\mu \delta^3(\mathbf{r} - \mathbf{l}), \quad (29)$$

namely, a Dirac string field [120, 124]. Eq. (27) shows that the correlation function of the U(1) phase variables maps to the ratio between the dual theory's partition functions with and without the Dirac string field.

Eq. (21) suggests phase transitions induced by a change of the fugacity parameter, similar to those in the Coulomb loop gas models. Nonetheless, the non-local nature of the S_t term hinders the systematic analysis of the dual continuum model. In the following subsection, we derive an alternative formulation of the dual action by discretizing the continuum theory on a cubic lattice. This approach introduces an emergent U(1) phase variable $\psi(\mathbf{r})$, yielding a fully local action in terms of $\Theta(\mathbf{r})$ and $\psi(\mathbf{r})$.

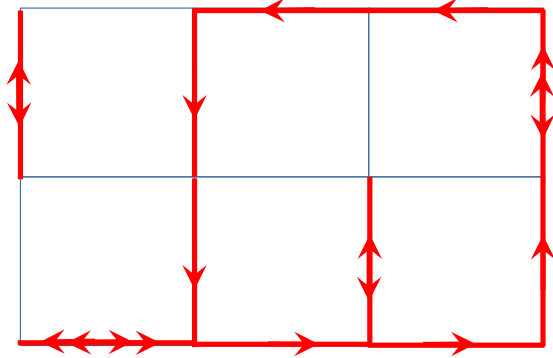


FIG. 1. An example of closed-loop graphs with direction that have time-reversal pairs on the same links. For this closed-loop graph, the RHS of Eq. (32) gives a weight $t^{18}/(2!2!2!)$, while the LHS of Eq. (32) gives a weight t^{18} . The additional weight can be regarded as an additional fugacity for the higher vorticity.

B. Dual lattice model

To this end, let us begin with the partition function after the h -field integration,

$$\begin{aligned} Z &= \int D[\Theta] e^{-S_{u(1)} - S_{su(N)}} \\ &\int D[\phi_v] \int D[P] e^{-i \int d^3r \text{Tr}[\Theta(\mathbf{r}) \cdot \mathbf{J}(\mathbf{r})]}. \quad (30) \end{aligned}$$

We first discretize the coupling term between $\mathbf{J}(\mathbf{r})$ and $\Theta(\mathbf{r})$ on a cubic lattice,

$$\begin{aligned}
& \int \mathcal{D}[\phi_v] \int \mathcal{D}[P] e^{-i \int d^3 r \text{Tr}[\Theta(\mathbf{r}) \cdot \mathbf{J}(\mathbf{r})]} = 1 + \\
& \sum_{n=1}^{\infty} \frac{1}{n!} \prod_{j=1}^n \left(\int dl_j t^{l_j} \int d^3 R_j \int_{\lambda \in [0, l_j]} \mathcal{D}\Omega_j(\lambda) \int_{r_j \in C_j} \mathcal{D}|p(r_j)\rangle \right) \exp \left[-2\pi i \sum_{j=1}^n \oint_{C_j} dl_{\mu} \sum_{a=0}^{N^2-1} \theta_{\mu}^a(\mathbf{l}) \langle p(\mathbf{l}) | T^a | p(\mathbf{l}) \rangle \right] \\
& \rightarrow 1 + \sum_{\text{all closed loops}} t^L \prod_{m \in \text{all the loops}} \left(\int \mathcal{D}|p_m\rangle \right) \exp \left[-2\pi i \sum_{n, \mu \in \text{all the loops}} \sum_{a=0}^{N^2-1} \theta_{n, \mu}^a \langle p_n | T^a | p_n \rangle \right]. \quad (31)
\end{aligned}$$

On the right-hand side (RHS), cubic lattice points are coordinated by an integer-valued 3D index $m \equiv (m_x, m_y, m_z)$. A closed vortex loop with direction is formed by connecting nearest-neighbor cubic lattice points. $\mathbb{C}\mathbb{P}^{N-1}$ vector $|p_m\rangle$ is defined at cubic lattice point m . Magnetic gauge field $\theta_{m, \mu}^a$ ($a = 0, 1, \dots, N^2 - 1$) resides on a nearest-neighbor link between m and $m + \hat{\mu}$ ($\mu = x, y, z$), with a convention of an antisymmetric condition, $\theta_{m, -\mu}^a = -\theta_{m, \mu}^a$. Here $\hat{\mu}$ is the unit vector along the $+\mu$ axis. The first summation in the RHS (sum over all closed loops) is over all possible configurations of directed loops on the cubic lattice. In summation, two vortex lines can share links as well as lattice points. The second summation in the RHS (sum over $n, \mu \in$ all the loops) is over all links along directed loops. If loops have a link from n to $n + \hat{x}$ and to $n - \hat{x}$, the summand includes $\theta_{n, x}^a \langle p_n | T^a | p_n \rangle$ and $-\theta_{n-\hat{x}, x}^a \langle p_{n-\hat{x}} | T^a | p_{n-\hat{x}} \rangle$, respectively.

The first product in the RHS (product over $m \in$ all the loops) is over all lattice points along directed loops. When a lattice point is traversed by the directed loops q times, the product has multiple integrals over q distinct $\mathbb{C}\mathbb{P}^{N-1}$ vectors. Notably, the first summation in the RHS counts those directed loops with time-reversal pairs on the same links, where the path traverses the same links both in forward and backward directions (see Fig. 1): the links with time-reversal pairs are regarded as having fine loop structures smaller than the lattice constant. L in the RHS denotes the total number of links that constitute all the vortex loops.

The sum over all directed-loop configurations on the cubic lattice can be taken by multiple integrals over $U(1)$ phase variables ψ_m defined on all cubic lattice sites,

$$\begin{aligned}
& 1 + \sum_{\text{all closed loops}} t^L \prod_{m \in \text{all the loops}} \left(\int \mathcal{D}|p_m\rangle \right) \exp \left[-2\pi i \sum_{n, \mu \in \text{all the loops}} \sum_{a=0}^{N^2-1} \theta_{n, \mu}^a \langle p_n | T^a | p_n \rangle \right] \\
& \simeq \prod_m \left(\int_0^{2\pi} \frac{d\psi_m}{2\pi} \right) \sum_{L=0}^{\infty} \frac{t^L}{L!} \left(\sum_m \sum_{\mu=x, y, z} \sum_{\sigma=\pm} \int \mathcal{D}|p_m\rangle \exp \left[i\sigma(\psi_{m+\hat{\mu}} - \psi_m + 2\pi \sum_{a=0}^{N^2-1} \theta_{m, \mu}^a \langle p_m | T^a | p_m \rangle) \right] \right)^L. \quad (32)
\end{aligned}$$

On the RHS, the product and sum of m are over all the cubic lattice points in the system. Suppose that the system has M cubic lattice points. Then, $(\dots)^L$ in the RHS can be expanded into $(M \times 3 \times 2)^L$ terms, each involving multiple integrals over L distinct $\mathbb{C}\mathbb{P}^{N-1}$ vectors (Here M , 3 and 2 come from the sums of m , μ and σ , respectively). Each term can be represented by a directed graph composed of nearest-neighbor links with arrows, where a link with an arrow from m to $m + \hat{\mu}$ and to $m - \hat{\mu}$ represents a phase factor of $\exp[i(\psi_{m+\hat{\mu}} - \psi_m + \dots)]$ and $\exp[-i(\psi_m - \psi_{m-\hat{\mu}} + \dots)]$, respectively. The multiple integrals over ψ_m fields of all the lattice points eliminate most of the $(M \times 3 \times 2)^L$ terms, except for those terms represented by closed directed-loop graphs, e.g., Fig. 1.

Thereby, both the RHS and LHS of Eq. (32) count exactly the same closed-loop graphs with the same phase factors. The caveat is that while the LHS always gives t^L for a closed directed-loop graph with L links, the RHS gives an additional weight for some closed directed-loop graphs due to combinatorial factors. Namely, when a graph traverses the same link in the same direction r times, the RHS gives the additional weight factor of $1/r!$ from the link. Since such an additional weight can be interpreted as additional core energies for vortex segments with *higher* vorticity, the RHS may as well be regarded as the partition function with a different lattice regularization. Given the RHS of Eq. (32) as the lattice model

of $\int D[\phi_v] \int D[P] e^{-i \int d^3 r \text{Tr}[\Theta(\mathbf{r}) \cdot \mathbf{J}(\mathbf{r})]}$, we finally obtain,

$$\begin{aligned} & \int D[\phi_v] \int D[P] e^{-i \int d^3 r \text{Tr}[\Theta(\mathbf{r}) \cdot \mathbf{J}(\mathbf{r})]} \\ & \rightarrow \prod_m \left(\int_0^{2\pi} \frac{d\psi_m}{2\pi} \right) \exp \left[2t \sum_m \sum_{\mu=x,y,z} \int d|p_m\rangle \right. \\ & \left. \cos \left(\psi_{m+\hat{\mu}} - \psi_m + 2\pi \sum_{a=0}^{N^2-1} \theta_{m,\mu}^a \langle p_m | T^a | p_m \rangle \right) \right]. \quad (33) \end{aligned}$$

Let us next discretize the Maxwell action on the cubic lattice [120, 124]. On the lattice, the curl of the magnetic gauge field $(\nabla \times \theta^a)_{\bar{m},\mu}$ is defined on a dual lattice link connecting dual cubic lattice sites \bar{m} and $\bar{m} + \hat{\mu}$. The curl represents an oriented sum of $\theta_{m,\nu}^a$ along edges of a plaquette intersected by the dual lattice link, e.g.

$$\begin{aligned} (\nabla \times \theta^a)_{\bar{m},x} &= -\theta_{\bar{m}+\hat{x}/2-\hat{y}/2+\hat{z}/2,y}^a + \theta_{\bar{m}+\hat{x}/2+\hat{y}/2-\hat{z}/2,z}^a \\ &+ \theta_{\bar{m}+\hat{x}/2-\hat{y}/2-\hat{z}/2,y}^a - \theta_{\bar{m}+\hat{x}/2-\hat{y}/2-\hat{z}/2,z}^a. \quad (34) \end{aligned}$$

To sum up, the partition function in the saddle-point manifold is mapped to the following dual lattice model,

$$Z \equiv \int D[\Theta] D[\psi] \exp[-S_{\text{u}(1)} - S_{\text{su}(N)} - S_t], \quad (35)$$

$$S_{\text{u}(1)} = \frac{2\pi}{\sigma + Nc} \sum_{\bar{m},\mu} \left[(\nabla \times \theta^0)_{\bar{m},\mu} - \frac{\sqrt{N}}{8\pi} \chi_\mu \right]^2, \quad (36)$$

$$S_{\text{su}(N)} = \frac{2\pi}{\sigma} \sum_{\bar{m},\mu} \sum_{a=1}^{N^2-1} (\nabla \times \theta^a)_{\bar{m},\mu}^2, \quad (37)$$

$$\begin{aligned} S_t &= -2t \sum_{m,\mu} \int d|p_m\rangle \cos \left[\psi_{m+\hat{\mu}} - \psi_m \right. \\ & \left. + 2\pi \sum_{a=0}^{N^2-1} \theta_{m,\mu}^a \langle p_m | T^a | p_m \rangle \right]. \quad (38) \end{aligned}$$

As in the dual continuum theory, the correlation function of the U(1) phase variable, Eq. (11), also maps to the ratio between the dual theory's partition functions with and without the Dirac string field \mathbf{v}^D [120, 124],

$$\langle e^{i[\phi(\mathbf{r}_1) - \phi(\mathbf{r}_2)]} \rangle = \frac{Z[\mathbf{v}^D]}{Z[0]}, \quad (39)$$

and

$$Z[\mathbf{v}^D] = \int D[\Theta] D[\psi] \exp \{ -S_{\text{u}(1)}[\mathbf{v}^D] - S_{\text{su}(N)} - S_t \}, \quad (40)$$

$$\begin{aligned} S_{\text{u}(1)}[\mathbf{v}^D] &= \\ & \frac{2\pi}{\sigma + Nc} \sum_{\bar{m},\mu} \left[(\nabla \times \theta^0)_{\bar{m},\mu} - \frac{\sqrt{N}}{8\pi} \chi_\mu + \sqrt{N} v_{\bar{m},\mu}^D \right]^2. \quad (41) \end{aligned}$$

On the lattice, the Dirac string field v^D is depicted by a directed line from dual cubic lattice site \bar{m}_1 (that corresponds to \mathbf{r}_1) to \bar{m}_2 (that corresponds to \mathbf{r}_2). The open line is formed by connecting nearest-neighbor dual-cubic-lattice links. $v_{\bar{m},\mu}^D$ in Eq. (41) takes +1 and -1, when a link from \bar{m} to $\bar{m} + \hat{\mu}$ is traversed by the directed line in the same and opposite direction, respectively. Otherwise, $v_{\bar{m},\mu}^D = 0$.

The dual lattice model for $N = 1$ portrays the magnetostatics of a U(1) type-II superconductor subjected to an external magnetic field along χ [23, 120, 124]. In the model, ψ_m represents the U(1) phase of the superconducting order parameter on the cubic lattice site m . The U(1) phase ψ_m couples with the U(1) gauge field θ_m^0 through the magnetic coupling. In the dual model, the fugacity parameter t becomes the Josephson coupling constant, and the 1D weak topological term χ becomes the external magnetic field. When $\chi = 0$, the disordered phase, characterized by divergent fugacity parameter t , maps to the superconducting phase where the large Josephson coupling t breaks the global U(1) gauge symmetry spontaneously, and the U(1) gauge field acquires a finite mass via the Anderson-Higgs mechanism [105, 106]. Conversely, the ordered phase, with vanishing fugacity parameter t , maps to the normal phase, where the fluctuation of the U(1) gauge field, favored by the entropic effect but constrained by the Maxwell action, completely suppresses the superconducting order.

A similar mapping of the phase diagram is also expected for general N , as the models share the same local U(1) gauge symmetry,

$$\psi_m \rightarrow \psi_m - \varphi_m, \quad \theta_{m,\mu}^0 \rightarrow \theta_{m,\mu}^0 + \frac{2\pi \Delta_\mu \varphi_m}{\sqrt{N}}, \quad (42)$$

with $\Delta_\mu \varphi_m \equiv \varphi_{m+\hat{\mu}} - \varphi_m$. In the next section, we first discuss a mean-field picture of the large- t (superconducting, Meissner) phase for general N .

V. ANDERSON LOCALIZATION IN CHIRAL UNITARY CLASS

When the large t induces the spontaneous symmetry breaking of the global U(1) gauge symmetry, an associated gapless Goldstone mode is absorbed by the U(1) gauge field, and the gauge field acquires a finite mass. To see this mass acquisition, let us expand the Josephson coupling term up to the second order in the gauge field fluctuation $\delta\Theta(\mathbf{r}) = \sum_{a=0}^{N^2-1} \delta\theta^a(\mathbf{r}) T^a$,

$$\delta S = 2\pi \int d^3 r \left[\frac{(\nabla \times \delta\theta^0)^2}{\sigma + Nc} + \sum_{a=1}^{N^2-1} \frac{(\nabla \times \delta\theta^a)^2}{\sigma} \right] \quad (43)$$

$$+ 4\pi^2 t \int d^3 r \int |p(\mathbf{r})\rangle \text{Tr}^2[\delta\Theta(\mathbf{r}) P(\mathbf{r})]. \quad (44)$$

With use of a formula [95, 103]

$$\begin{aligned} & \int d|p\rangle \text{Tr}(AP) \text{Tr}(BP) \\ &= \frac{\pi^{N-1}}{N(N+1)\Gamma(N)} [\text{Tr}(AB) + \text{Tr}(A) \text{Tr}(B)], \end{aligned} \quad (45)$$

the integral over $p(\mathbf{r})$ yields a decoupling among the N^2 gauge fields,

$$\begin{aligned} \delta S &= 2\pi \int d^3r \left[\frac{(\nabla \times \delta\theta^0)^2}{\sigma + Nc} + \frac{2\pi^N t}{N\Gamma(N)} (\delta\theta^0)^2 \right] \\ &+ 2\pi \int d^3r \sum_a \left[\frac{(\nabla \times \delta\theta^a)^2}{\sigma} + \frac{2\pi^N t}{N(N+1)\Gamma(N)} (\delta\theta^a)^2 \right]. \end{aligned} \quad (46)$$

Notably, both U(1) and SU(N) gauge fields acquire finite mass, while the two masses converge to the same finite constant in the replica limit ($N \rightarrow 0$). The mass of the U(1) gauge field gives an energy penalty to the partition function with the Dirac string field, $Z[v^D]$, in comparison to the partition function without the Dirac string field, and the energy penalty is proportional to the distance between the magnetic monopole and antimonopole. Thus, the U(1) phase correlation function given by Eq. (39) decays exponentially in the distance $|\mathbf{r}_1 - \mathbf{r}_2|$ for general integer N . In the limit of $N \rightarrow 0$, such a short-ranged correlation of the U(1) phase variables is consistent with the Anderson insulator in the chiral NLSM. When the mass is absent ($t = 0$), the action is given only by the Maxwell term, where an energy penalty that $Z[v^D]$ pays relative to $Z[0]$ in Eq. (39) is given by the $1/r$ Coulomb interaction between the magnetic charges. Thereby, the correlation function remains finite even for larger $|\mathbf{r}_1 - \mathbf{r}_2|$, which is consistent with the diffusive metal phase in the chiral NLSM.

In the next section, we will develop a mean-field theory of the superconducting phase of the U(N) lattice superconductor model for general N . We will show that the

theory in the replica limit ($N \rightarrow 0$) has a phase transition from a large- t phase (superconducting, Meissner / Anderson localized) phase to a small- t ordered phase (normal, Maxwell / diffusive metal) phase.

A. Variational analysis

To gain a mean-field gap equation for the Higgs mass for the gauge field, we use a variational method and study the continuum limit of the action $S_{u(1)} + S_{su(N)} + S_t$:

$$\begin{aligned} S &= \int d^3r \left\{ 2\pi \left[\frac{(\nabla \times \theta^0)^2}{\sigma + Nc} + \sum_{a=1}^{N^2-1} \frac{(\nabla \times \theta^a)^2}{\sigma} \right] \right. \\ &\quad \left. - 2t \cos \left[\sum_{a=0}^{N^2-1} \theta_\mu^a(\mathbf{r}) \langle p(\mathbf{r}) | T^a | p(\mathbf{r}) \rangle \right] \right\}. \end{aligned} \quad (47)$$

Here the spatial gradient $\nabla_\mu \psi(\mathbf{r})$ of the superconducting phase is already absorbed into the U(1) gauge field, $\theta_\mu^0(\mathbf{r}) \rightarrow \theta_\mu^0(\mathbf{r}) + \nabla_\mu \psi(\mathbf{r})$. Based on a variational principle, we search for a trial action \bar{S} that minimizes a variational free energy $F \equiv \langle S - \bar{S} \rangle_{\bar{S}} - \ln \bar{Z}$, where the average $\langle \dots \rangle_{\bar{S}}$ is taken with a weight of $\exp(-\bar{S})$, and \bar{Z} is the partition function of the trial action. From Eq. (46) in the replica limit, we assume the following form of the trial action,

$$\begin{aligned} \bar{S} &= 2\pi \int d^3r \left\{ \left[\frac{(\nabla \times \theta^0)^2}{\sigma + Nc} + m^2 (\theta^0)^2 \right] \right. \\ &\quad \left. + \sum_{a=1}^{N^2-1} \left[\frac{(\nabla \times \theta^a)^2}{\sigma} + m^2 (\theta^a)^2 \right] \right\}, \end{aligned} \quad (48)$$

where the Higgs mass m plays the role of a variational parameter. F as a function of m can be calculated for general N . Notably, F thus calculated goes to zero in the replica limit, so that $f \equiv \lim_{N \rightarrow 0} F/(NV)$ corresponds exactly to $-\langle \ln \mathcal{Z} \rangle_{\text{dis}}/V$ in Eq. (1) (see Appendix C). f is calculated as a function of m ,

$$f(m) = -\frac{6t}{\pi} \exp \left\{ -\frac{\Lambda^3 \Lambda^3 + m \left[3\sqrt{\sigma} \Lambda^2 + m \left(2c\Lambda + 5\sigma\Lambda + 3m\sigma^{\frac{3}{2}} \right) \right]}{48 m^2 (\Lambda + \sqrt{\sigma}m)^3} \right\} + \frac{1}{8\pi} \frac{c\sqrt{\sigma}m^3 \Lambda^3}{(\Lambda + m\sqrt{\sigma})^3}. \quad (50)$$

where Λ is the UV cutoff for 3D momentum integrals in the calculation. We use a soft momentum cutoff for the 3D integrals; Λ^{-1} can be regarded as a lattice constant.

The first and second terms of $f(m)$ decrease and increase monotonically in increasing m , respectively, so that a competition between the two terms leads to a phase transition between the $m \neq 0$ phase [Anderson localized phase] and $m = 0$ phase [diffusive metal phase]. In fact,

the entropic effect associated with the gauge field fluctuations, that comes from $-\ln \bar{Z}$, is encoded in an increasing function of m in the second term, while internal energy that comes from $\langle S - S_0 \rangle_{\bar{S}}$ decreases in m , e.g. the first term. The critical value t_c of t is calculated for different values of σ and c [Fig. 2(b)], and the free energy density f is plotted as functions of m for $t > t_c$ and $t < t_c$. When the fugacity parameter t is below the critical value t_c , the

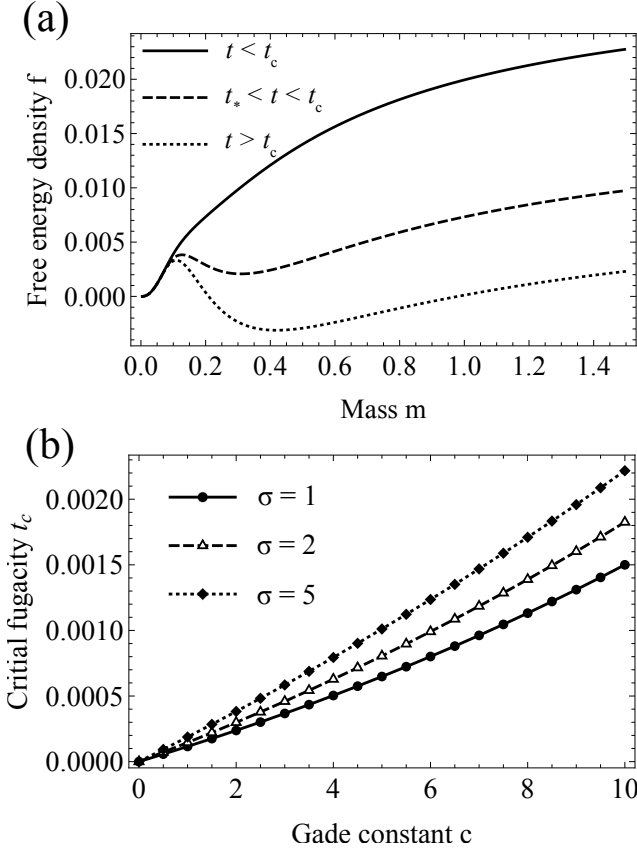


FIG. 2. (a) variational Free energy density f as a function of the Higgs mass at $\sigma = c = 80$ [for the $\chi = 0$ case]. Lattice constant Λ^{-1} is set as the unit. f has a single minimum at $m = 0$ for $t < t_*$, two local minima at $m = 0$ and at $m \neq 0$ for $t_* < t$. The two minima of f are degenerate at $t = t_c$, while for $t_c < t$, the global minimum of f is at $m \neq 0$. (b) Critical fugacity t_c for different conductivity σ and Gade constant c .

global minimum of f is at $m = 0$; when t is above t_c , the global minimum of f appears at $m \neq 0$. Notably, the function f at $t = t_c$ has two minima at $m = 0$ and at $m \neq 0$ [Fig. 2(a)].

The Anderson transition in the 3D chiral unitary class is a second-order phase transition [99, 102], and the first-order transition suggested by the two minima of the trial function is an artifact of the variational approximation. The approximation may underestimate the fluctuations of the superconducting phase and magnetic gauge fields. A similar first-order phase transition was also predicted by a mean-field analysis of the Anderson-Higgs model [124].

VI. QUASILOCALIZATION IN CHIRAL UNITARY CLASS

In the presence of χ , the lattice model of U(1) type-II superconductors exhibits a two-step phase transition, where an intermediate mixed phase emerges between the normal (Maxwell) and superconducting (Meissner) phases.

In this mixed phase, the system is permeated by a dense array of magnetic flux lines aligned along the $\chi \parallel z$ direction, spaced at finite intervals in the x - y plane [107–109].

In the mixed phase, the monopole-field correlation function, Eq. (39), remains finite for large $|\mathbf{r}_1 - \mathbf{r}_2|$ in the parallel geometry ($\mathbf{r}_1 - \mathbf{r}_2 \parallel z$ axis), while it decays exponentially with the distance in the perpendicular geometry ($\mathbf{r}_1 - \mathbf{r}_2 \perp z$ axis). This behavior arises because the Dirac string field \mathbf{v}^D emanating from the magnetic monopole to antimonopole in the parallel geometry is trapped inside one of the magnetic flux lines near \mathbf{r}_1 and \mathbf{r}_2 . As a result, the additional energy penalty that $Z[\mathbf{v}^D]$ incurs relative to $Z[0]$ is given only by the Coulomb interaction between the two magnetic charges, which vanishes as $|\mathbf{r}_1 - \mathbf{r}_2| \rightarrow \infty$. In contrast, the Dirac string field in the perpendicular geometry is inevitably exposed to some superconducting region, and the region is proportional to $|\mathbf{r}_1 - \mathbf{r}_2|$. Consequently, the additional energy penalty scales linearly with $|\mathbf{r}_1 - \mathbf{r}_2|$, leading to an exponential decay of the U(1) phase correlation function Eq. (39) along the perpendicular direction.

A similar phase transition from the normal phase to the intermediate mixed phase is also expected in the U(N) type-II superconductors for general N . When t is small or both σ and c are large, the superconducting phase is disordered, and the Josephson couplings vanish completely due to the fluctuations of the ψ field and gauge fields. When t is large or both σ and c are small, the internal energy dominates the entropic effect, and the system chooses to take the saddle-point solution(s) of Eq. (35). The global energy minimum of $S_{u(1)}$ is given by

$$\bar{\theta}_{m,\mu}^0 = \Delta_\mu \varphi_m + \frac{\sqrt{N}}{8\pi} A_{m,\mu}. \quad (51)$$

Here $\Delta_\mu \varphi_m \equiv \varphi_{m+\hat{\mu}} - \varphi_m$ is a longitudinal (rotation-free) component of the U(1) gauge field $\bar{\theta}_{m,\mu}^0$, and an external magnetic gauge potential \mathbf{A} satisfies $(\nabla \times \mathbf{A})_{\bar{m},\hat{\mu}} = \chi \delta_{\mu,z}$. The energy minimum of $S_{su(N)}$ can be achieved by the uniform su(N) gauge field,

$$\bar{\theta}_{m,\hat{\mu}}^{a \neq 0} = 0. \quad (52)$$

With Eqs. (51,52), S_t is minimized by

$$\bar{\psi}_{m+\hat{\mu}} - \bar{\psi}_m + \frac{2\pi \Delta_\mu \varphi_m}{\sqrt{N}} + \frac{A_{m,\hat{\mu}}}{4} = 2\pi \mathbb{Z}. \quad (53)$$

For $\chi = 0$, $\bar{\psi}_m = -2\pi \varphi_m / \sqrt{N}$ realizes Eq. (53) for all $\mu = x, y, z$ and m . For general values of χ , however, Eq. (53) cannot be simultaneously satisfied for all links. Namely, a line integral of Eq. (53) around a cubic-lattice plaquette in the x - y plane yields $\chi/4$ from the right-hand side, while it gives 8π times integers from the left-hand side. On the other hand, Eq. (53) for $\mu = z$ can be simultaneously satisfied for all m , as $A_{m,z} = 0$. Accordingly, the system may choose a phase where the U(1) superconducting phase variable preserves its coherence along $\chi \parallel z$, while the Josephson couplings within the x - y plane are destroyed

completely by the fluctuation of the ψ field. In such a phase, the cos terms along z links can be replaced by a quadratic fluctuation around its saddle point, yielding the following effective action,

$$S_{\text{quasi}} = 2\pi \int d^3r \left[\frac{(\nabla \times \delta\theta^0)^2}{\sigma + Nc} + \frac{2t\pi^N}{N\Gamma(N)} (\delta\theta_z^0)^2 \right] \quad (54)$$

$$+ 2\pi \int d^3r \sum_{a=1}^{N^2-1} \left[\frac{(\nabla \times \delta\theta^a)^2}{\sigma} + \frac{2t\pi^N}{N(N+1)\Gamma(N)} (\delta\theta_z^a)^2 \right], \quad (55)$$

with $\theta^a = \bar{\theta}^a + \delta\theta^a$. Notably, only the longitudinal component $\delta\theta_z^a$ of the gauge fields acquires a finite mass, while the transverse components $\delta\theta_\mu^a$ ($\mu = x, y$) do not. In such a phase, the introduction of the Dirac string field along x or y directions incurs an energy penalty that is

proportional to the string length, resulting in an exponential decay of the U(1) phase correlation along the x - y direction. Conversely, the Dirac string field along $\chi \parallel z$ is free from the mass so that the U(1) phase variable retains its coherence along χ . This extremely anisotropic U(1) phase coherence is consistent with the phenomenology of the quasi-localized phase in the chiral symmetric systems with the 1D weak band topology [102, 103].

The above mean-field description also suggests that the intermediate quasi-disordered phase in the Coulomb loop gas model with finite χ must be characterized by divergent fugacity parameter t_z for vortex loop segment polarized along $\chi \parallel z$, and vanishing fugacity parameter t_\perp for vortex loop segment polarized along the other directions. In fact, the mean-field action is consistent with a superconductor model with spatially anisotropic Josephson couplings, $t_z \neq t_\perp = t_x = t_y$,

$$Z = \int D[\Theta] \int D[\psi] \exp[-S_{\text{u}(1)} - S_{\text{su}(N)}] \sum_{L=0}^{\infty} \frac{1}{L!} \left(\sum_m \sum_{\mu=x,y,z} \sum_{\sigma=\pm} \int d|p_m\rangle t_\mu \exp \left[i\sigma(\psi_{m+\hat{\mu}} - \psi_m + 2\pi \sum_{a=0}^{N^2-1} \theta_{m,\mu}^a \langle p_m | T^a | p_m \rangle) \right] \right)^L. \quad (56)$$

Thereby, Eq. (55) can be regarded as a mean-field action for a phase with divergent t_z , and vanishing t_\perp . Notably, in the Coulomb loop gas model, $\ln t_z$ and $\ln t_\perp$ are nothing but chemical potentials of the vortex loop segment polarized along $\chi \parallel z$ and the loop segment polarized along the other two directions, respectively. Thus, a transition from ordered (diffusive metal) to quasilocalized (quasilocalized) phase in the Coulomb loop gas model can be regarded as a topological transition driven by the spatial proliferation of *polarized* vortex loops.

VII. SUMMARY

In this paper, we argue that vortex loop excitations drive the 3D Anderson transition in chiral symmetry classes, where an eigenvalue of the NLSM matrix-formed field variable Q permits the vortex-loop solutions as saddle-point configurations of the NLSM. Using an analogy to 3D magnetostatics in the presence of quantized electric current loops, we argue that the Anderson transition in chiral symmetry classes is driven by a condensation of the vortex loop excitations (quantized electric current loops). To elaborate on this picture, we further introduce a cubic-lattice model of U(N) type-II superconductors as

a dual representation of the NLSM in the chiral unitary class. By analyzing this lattice model by a variational method, we construct a mean-field theory of the 3D Anderson transition in the chiral unitary class. In the mean-field description, the metal phase with gapless diffusion mode becomes a normal (Maxwell) phase, where the Maxwell action controls the fluctuation of the gapless magnetic gauge field. Meanwhile, the localized phase is described as a superconducting (Meissner) phase with broken global U(1) gauge symmetry, where the gauge field acquires a finite mass via the Anderson-Higgs mechanism. Our dual representation also demonstrates that the 1D weak topology term in the 3D chiral NLSM becomes an external magnetic field in the 3D type-II superconductor model, where the quasi-localized phase in chiral symmetry classes shares a unified theoretical description with the mixed phase in the 3D superconductor.

ACKNOWLEDGMENTS

We thank Lingxian Kong, Yeyang Zhang, and Zhenyu Xiao for the discussions. The work was supported by the National Basic Research Programs of China (No. 2024YFA1409000) and the National Natural Science Foundation of China (No. 12074008 and No. 12474150).

Appendix A: Derivation of the nonlinear sigma model

A Hamiltonian H with chiral symmetry, $\sigma_z H \sigma_z = -H$, is given by a two-by-two block off-diagonal form, $H = (h_0 + V)\sigma_+ + (h_0^\dagger + V^\dagger)\sigma_-$, where h_0 and V are $M \times M$ non-Hermitian matrices. h_0 is a disorder-free tight-binding matrix. V is a diagonal matrix whose diagonal elements V_r are random complex numbers obeying the Gaussian distribution function with $\langle V_r \rangle_{\text{dis}} = 0$ and $\langle V_r^* V_{r'} \rangle_{\text{dis}} = \gamma^2 \delta_{rr'}$. A Green's function $G(z; r, r') = \langle r | (z - H)^{-1} | r' \rangle$ and its products are generated from a partition function,

$$\mathcal{Z} = \int d[\psi] \exp[-\psi^\dagger(z - H)\psi] = \int d[\psi] \exp[-\psi^\dagger(z - H)\sigma_x\psi], \quad (\text{A1})$$

with $\psi \equiv (\psi_+, \psi_-)^T$ and $\psi^\dagger \equiv (\psi_+^\dagger, \psi_-^\dagger)$. Here \pm is the chiral index associated with the two-by-two block-off diagonal structure [95, 103, 115]. The right-hand side is due to $\det \sigma_x = 1$. The Green's function and its product are obtained from derivatives of the partition function \mathcal{Z} with respect to a source field J , e.g.

$$G(z; r, r') = \frac{\partial \ln \mathcal{Z}}{\partial J_{r,r'}}. \quad (\text{A2})$$

As the derivatives and the disorder average commute with each other, we have only to calculate $\langle \ln \mathcal{Z} \rangle_{\text{dis}}$. To calculate $\langle \ln \mathcal{Z} \rangle_{\text{dis}}$, we use the replica trick,

$$\ln \mathcal{Z} = \lim_{N \rightarrow 0} \frac{\mathcal{Z}^N - 1}{N}, \quad (\text{A3})$$

where \mathcal{Z}^N is a partition function of N replicated fermion field $\psi_m \equiv (\psi_{m,+}, \psi_{m,-})^T$ ($m = 1, \dots, N$). The Gaussian average of \mathcal{Z}^N induces an attractive interaction among the replicated ψ -fields,

$$\langle \mathcal{Z}^N \rangle_{\text{dis}} = \int d[\psi] \exp \left[- \sum_{n=1}^N \psi_n^\dagger (z - H_0) \sigma_x \psi_n + \frac{\gamma^2}{2} \sum_{m,n=1}^N \sum_{r=1}^M \psi_{m,+}^* \psi_{m,+} \psi_{n,-}^* \psi_{n,-} \right], \quad (\text{A4})$$

with $H_0 = h_0 \sigma_+ + h_0^\dagger \sigma_-$. H_0 is diagonal in the replica index (n) and independent of the replica index n .

1. Self-consistent Born approximation

The attractive interaction is further decomposed by the use of the Hubbard-Stratonovich (HS) transformation,

$$\begin{aligned} & \exp \left[\frac{\gamma^2}{2} \sum_{m,n,r} \psi_{m,+}^* \psi_{m,+} \psi_{n,-}^* \psi_{n,-} \right] \\ &= \int d[Q] \exp \left[-\frac{1}{2\gamma^2} \text{Tr}(Q^\dagger Q) + i \left(\psi_+^\dagger Q \psi_- + \psi_-^\dagger Q^\dagger \psi_+ \right) \right]. \end{aligned} \quad (\text{A5})$$

Here, the HS field (Q field) takes the form of an N by N matrix. The Q field is diagonal in the lattice-site index r , while it is dependent on r . The partition function of the N replicated fields is given by

$$\langle \mathcal{Z}^N \rangle_{\text{dis}} = \int D[Q, \psi] \exp \left[-\frac{1}{2\gamma^2} \text{Tr}(Q^\dagger Q) - \psi^\dagger \begin{pmatrix} z - iQ & -h_0 \\ -h_0^\dagger & z - iQ^\dagger \end{pmatrix} \sigma_x \psi \right]. \quad (\text{A6})$$

An integration of the fermion ψ -field yields the partition function for the auxiliary Q field,

$$\begin{aligned} \langle \mathcal{Z}^N \rangle_{\text{dis}} &= \int D[Q] \exp \left[-\frac{1}{2\gamma^2} \text{Tr}(Q^\dagger Q) + \text{Tr} \ln \begin{pmatrix} z - iQ & -h_0 \\ -h_0^\dagger & z - iQ^\dagger \end{pmatrix} \right], \\ &\equiv \int D[Q] \exp[-S[Q, z]]. \end{aligned} \quad (\text{A7})$$

Here, the trace on the right-hand side is taken over the chiral index (\pm), replica index (m, n), and the lattice site index (r).

Self-consistent Born solution is a saddle-point solution Q of the action $S[Q, z]$. For simplicity, we will not explore general structures of the saddle-point solutions of specific tight-binding Hamiltonians h_0 in the chiral unitary class. Instead, we assume a (commonly used) *ansatz* $Q = \lambda 1_{N \times N}$. Real and imaginary parts of λ physically mean an inverse of the mean free time and energy renormalization of diffusive particles, respectively. With periodic boundary conditions for h_0 , the action in the momentum space may become

$$S[\lambda 1_{N \times N}, z] = -\frac{NM}{2\gamma^2} \lambda^* \lambda + M \sum_k \text{Tr} \ln \begin{pmatrix} z - i\lambda & -h_0(\mathbf{k}) \\ -h_0^*(\mathbf{k}) & z - i\lambda^* \end{pmatrix}. \quad (\text{A8})$$

Here we assume that the eigenvalues of an M by M non-Hermitian matrix h_0 are given by complex values $h_0(\mathbf{k})$, where k takes M discrete values from the periodic boundary condition. The trace (Tr) on the right-hand side is taken over the chiral index. The stationary point is determined by

$$0 = \frac{\partial S}{\partial \lambda^*} = -\frac{NM}{2\gamma^2} \lambda + N \sum_k \text{Tr} \left[\begin{pmatrix} z - i\lambda & -h_0(\mathbf{k}) \\ -h_0^*(\mathbf{k}) & z - i\lambda^* \end{pmatrix}^{-1} \begin{pmatrix} 0 & 0 \\ 0 & -i \end{pmatrix} \right]. \quad (\text{A9})$$

The trace can be calculated as

$$\text{Tr} \left[\begin{pmatrix} z - i\lambda & -h_0(\mathbf{k}) \\ -h_0^*(\mathbf{k}) & z - i\lambda^* \end{pmatrix}^{-1} \begin{pmatrix} 0 & 0 \\ 0 & -i \end{pmatrix} \right] = \sum_k \frac{-i(z - i\lambda)}{(z - i\lambda)(z - i\lambda^*) - \epsilon_k^2}, \quad (\text{A10})$$

with $\epsilon_k^2 = |h_0(\mathbf{k})|^2 \geq 0$. The saddle-point equation reduces to

$$\lambda = -\frac{2i\gamma^2}{M} \sum_k \frac{z - i\lambda}{(z - i\lambda)(z - i\lambda^*) - \epsilon_k^2}. \quad (\text{A11})$$

In the thermodynamic limit, we may replace the k -sum by an energy integral with a density of states $\rho(\epsilon) \equiv \frac{1}{M} \sum_k \delta(\epsilon - \epsilon_k)$,

$$\lambda = -2i\gamma^2 \int_0^\infty d\epsilon \rho(\epsilon) \frac{z - i\lambda}{(z - i\lambda)(z - i\lambda^*) - \epsilon^2}. \quad (\text{A12})$$

Here, we set $z = 0$, because the chiral symmetry is respected exclusively by zero-energy eigenstates of H , and the Anderson transition in chiral symmetry class depends solely on the zero-energy Green's function $G(z = 0)$. The gap equation at $z = 0$ suggests either $\lambda = 0$ solution or $\lambda \neq 0$ solution that satisfies,

$$1 = 2\gamma^2 \int_0^\infty d\epsilon \frac{\rho(\epsilon)}{|\lambda|^2 + \epsilon^2}. \quad (\text{A13})$$

When $\rho(\epsilon) \simeq \epsilon^\alpha$ for $\epsilon \simeq 0$ and $\alpha \geq 1$, the gap equation for small γ has only $\lambda = 0$ solution (a solution of ballistic transport) [126, 127]. Otherwise, the gap equation generally has a $\lambda \neq 0$ solution (a solution of diffusive transport).

2. Nonlinear sigma model

The action at $z = 0$ has a continuous symmetry, and the $\lambda \neq 0$ solution has a degeneracy;

$$\langle \mathcal{Z}^N \rangle_{\text{dis}} = \int d[Q] \exp \left[-\frac{1}{2\gamma^2} \text{Tr} (Q^\dagger Q) + \text{Tr} \ln \begin{pmatrix} -iQ & -h_0 \\ -h_0^\dagger & -iQ^\dagger \end{pmatrix} \right]. \quad (\text{A14})$$

The action is invariant under the continuous transformation $Q \rightarrow U_1 Q U_2^\dagger$, with two N by N unitary matrices U_1 and U_2 that are independent of the spatial coordinate r . The symmetry dictates that the self-consistent Born (SCB) solution $Q = \lambda 1_{N \times N}$ must have degeneracy with $Q = \lambda U_1 U_2^\dagger$. For $U_1 = U_2$, they are identical. Thus, the degenerate SCB solutions form a manifold defined by a matrix group $U(N) \times U(N)/U(N) \cong U(N)$. The matrix group is called the Goldstone manifold. The group $U(N) \times U(N)$ in the numerator is called the symmetry group, while the group $U(N)$ in the denominator is called the stabilizer group.

Since the SCB solution breaks the continuous symmetry, the solution is accompanied by gapless Goldstone modes – diffusion mode. To describe the diffusion mode, let us take $Q = \lambda U$, where a N by N matrix U is diagonal in r but slowly varying in r . The partition function of the replicated fermion fields reduces to

$$\langle \mathcal{Z}^N \rangle_{\text{dis}} = \int d[U] \exp \left[-\frac{|\lambda|^2 MN}{2\gamma^2} + \text{Tr} \ln \begin{pmatrix} -i\lambda & -U^\dagger h_0 U \\ -h_0^\dagger & -i\lambda^* \end{pmatrix} \right]. \quad (\text{A15})$$

On the right-hand side, the r -dependent U does not commute with h_0 , while the r -independent U yields the SCB action, Eq. (A8). To extract energy cost from the r -dependency in U , one can exercise a gradient expansion around the SCB Green's function G_0^{-1} ,

$$\begin{aligned} \langle \mathcal{Z}^N \rangle_{\text{dis}} &= \exp[-S_{\text{scb}}] \int d[U] \exp \left[\text{Tr} \ln \left[1 + G_0 \begin{pmatrix} 0 & \Delta_U h_0 \\ 0 & 0 \end{pmatrix} \right] \right] \\ &= \exp[-S_{\text{scb}}] \int d[U] \exp \left[\text{Tr} \left[G_0 \begin{pmatrix} 0 & \Delta_U h_0 \\ 0 & 0 \end{pmatrix} \right] - \frac{1}{2} \text{Tr} \left[G_0 \begin{pmatrix} 0 & \Delta_U h_0 \\ 0 & 0 \end{pmatrix} G_0 \begin{pmatrix} 0 & \Delta_U h_0 \\ 0 & 0 \end{pmatrix} \right] + \dots \right] \\ &\equiv \exp[-S_{\text{scb}}] \int d[U] \exp[-S_{\text{NLSM}}[U]], \end{aligned} \quad (\text{A16})$$

with $S_{\text{scb}} \equiv S[\lambda 1_{N \times N}, z = 0]$ and $\Delta_U h_0 \equiv -U^\dagger h_0 U + h_0$. The SCB Green's function G_0 at the zero energy ($z = 0$) is given by,

$$G_0^{-1} = \begin{pmatrix} -i\lambda & -h_0 \\ -h_0^\dagger & -i\lambda^* \end{pmatrix}. \quad (\text{A17})$$

In the following, we deduce the form of $S_{\text{NLSM}}[U]$ based on symmetry arguments. Since $\Delta_U h_0 = 0$ for the r -independent U , $\Delta_U h_0$ must reduce to a linear combination of $U^{-1} \nabla_\mu U$ in the continuum limit ($\mu = x, y, \dots$). Possible scalar quantities one can construct out of $U^{-1} \nabla_\mu U$ and their products are $\text{Tr}[U^{-1} \nabla_\mu U]$, $\text{Tr}[U^{-1} \nabla_\mu U \cdot U^{-1} \nabla_\nu U]$, $\text{Tr}[U^{-1} \nabla_\mu U] \text{Tr}[U^{-1} \nabla_\nu U]$, and higher-order gradient terms [79, 80]. Suppose that a disordered system considered here has (statistical) mirror symmetries with respect to spatial directions except for z , e.g., $(x, y, z) \rightarrow (-x, y, z)$ or $(x, -y, z)$. The mirror symmetries forbid cross terms ($\mu \neq \nu$) in $\text{Tr}[U^{-1} \nabla_\mu U \cdot U^{-1} \nabla_\nu U]$ and $\text{Tr}[U^{-1} \nabla_\mu U] \text{Tr}[U^{-1} \nabla_\nu U]$. The symmetries also forbid $\text{Tr}[U^{-1} \nabla_\mu U]$ with $\mu = x, y$. Thus, up to the second order in the expansion, the symmetry-allowed form of S_{NLSM} is given by

$$S_{\text{NLSM}}[U] = - \int \frac{d^d r}{8\pi} \sum_\mu \left[\sigma_\mu \text{Tr} (U^{-1} \nabla_\mu U)^2 + c_\mu \text{Tr}^2 (U^{-1} \nabla_\mu U) - \chi \text{Tr} (U^{-1} \nabla_z U) \right]. \quad (\text{A18})$$

Notably, σ_μ and c_μ must be positive and χ must be real. Otherwise, the spatially uniform saddle-point solution $Q = \lambda 1_{N \times N}$ cannot be a local energy minimum of the action $S[Q, z]$. In the absence of any other statistical symmetries that change the sign of z , e.g. $(x, y, z) \rightarrow (x, y, -z)$, real-valued χ is generally finite.

Appendix B: Saddle-point equation of the nonlinear sigma model

In this Appendix, we derive a set of saddle-point equations of the chiral NLSM, Eqs (6,7,8), as well as Eq. (16). We also discuss a general feature of $P(\mathbf{r}) \equiv |p(\mathbf{r})\rangle \langle p(\mathbf{r})|$ that satisfies the saddle-point equations, and how the Poisson equation for $\phi(\mathbf{r})$ can be obtained from them. The derivation can be applied to all three chiral symmetry classes. $Q(\mathbf{r})$ in the chiral classes has unit complex numbers $e^{i\phi_n(\mathbf{r})}$ as its eigenvalues,

$$Q(\mathbf{r}) = \sum_{n=1}^N e^{i\phi_n(\mathbf{r})} |p_n(\mathbf{r})\rangle \langle p_n(\mathbf{r})|.$$

$|p_n(\mathbf{r})\rangle$ is a corresponding eigenvector. General saddle-point solutions of the NLSM could be obtained from its derivatives with respect to all eigenvalues and eigenvectors of the Q field. In saddle-point solutions thus obtained, each eigenvalue $e^{i\phi_n(\mathbf{r})}$ could have multiple vortex excitations separately. When such vortex excitations have no spatial overlap with one another, however, one may utilize an r -dependent basis change in such a way that only one eigenvalue

$e^{i\phi(\mathbf{r})}$ has all the vortex excitations, while the others do not. To introduce such a generic Q configuration as the saddle-point solution, we may use the following ansatz;

$$\begin{aligned} Q(\mathbf{r}) &= e^{i\psi(\mathbf{r})} + \left[e^{i\phi(\mathbf{r})} - e^{i\psi(\mathbf{r})} \right] |p(\mathbf{r})\rangle\langle p(\mathbf{r})| \\ &= e^{i\psi(\mathbf{r})} \left(1 + \left[e^{i\phi(\mathbf{r})-i\psi(\mathbf{r})} - 1 \right] |p(\mathbf{r})\rangle\langle p(\mathbf{r})| \right). \end{aligned} \quad (\text{B1})$$

In the ansatz, only one eigenvalue $e^{i\phi(\mathbf{r})}$, which an eigenstate $|p(\mathbf{r})\rangle$ belongs to, has vortex excitations, while the other eigenvalues $e^{i\psi(\mathbf{r})}$ are degenerate, and do not have any vortices. Since the overall factor $e^{i\psi(\mathbf{r})}$ in the right hand side can be absorbed into the spin-wave part of the Q field, we may also use Eq. (5) by replacing $e^{i\phi(\mathbf{r})-i\psi(\mathbf{r})}$ by $e^{i\phi(\mathbf{r})}$. From Eq. (5) with $P(\mathbf{r}) \equiv |p(\mathbf{r})\rangle\langle p(\mathbf{r})|$, we obtain

$$\begin{aligned} \nabla_\mu Q &= i\nabla_\mu \phi e^{i\phi} P + (e^{i\phi} - 1) \nabla_\mu P, \\ Q^{-1} \nabla_\mu Q &= i\nabla_\mu \phi P + 2(1 - \cos \phi) P \nabla_\mu P + (e^{i\phi} - 1) \nabla_\mu P. \end{aligned} \quad (\text{B2})$$

With the use of $\text{Tr}(P) = 1$, $\text{Tr}(\nabla_\mu P) = \nabla_\mu \text{Tr}(P) = 0$, $\text{Tr}(P \nabla_\mu P) = \text{Tr}(\nabla_\mu P P) = \frac{1}{2} \text{Tr}(\nabla_\mu P) = 0$, $P^2 = P$, $\nabla_\mu P P + P \nabla_\mu P = \nabla_\mu P$, and

$$\begin{aligned} \text{Tr}(P \nabla_\mu P)^2 &= \text{Tr}(\nabla_\mu P P \nabla_\mu P) - \text{Tr}(\nabla_\mu P P^2 \nabla_\mu P) = 0, \\ \text{Tr}(\nabla_\mu P)^2 &= 2 \text{Tr}(P \nabla_\mu P \nabla_\mu P), \end{aligned}$$

we obtain the following formulas,

$$\begin{aligned} \text{Tr}(Q^{-1} \nabla_\mu Q) &= i\nabla_\mu \phi, \\ \text{Tr}(Q^{-1} \nabla_\mu Q)^2 &= -(\nabla_\mu \phi)^2 - 2(1 - \cos \phi) \text{Tr}(\nabla_\mu P)^2. \end{aligned}$$

Thus, the action with the saddle-point ansatz, Eq. (5), is given by

$$S = \int \frac{d^3 r}{8\pi} \sum_\mu \left[(\sigma_\mu + c_\mu) (\nabla_\mu \phi)^2 + 2\sigma_\mu (1 - \cos \phi) \text{Tr}(\nabla_\mu P)^2 + i\chi_\mu \nabla_\mu \phi \right]. \quad (\text{B3})$$

Derivatives of Eq. (B3) with respect to the U(1) phase $\phi(\mathbf{r})$ and matrix elements of $P(\mathbf{r})$ give

$$\sum_\mu (\sigma_\mu + c_\mu) \nabla_\mu^2 \phi - \sum_\mu \sigma_\mu \sin \phi \text{Tr}(\nabla_\mu P)^2 = 0, \quad (\text{B4})$$

and

$$\sum_\mu \sigma_\mu (1 - \cos \phi) \nabla_\mu^2 P + \sum_\mu \sigma_\mu \sin \phi \nabla_\mu \phi \nabla_\mu P = 0, \quad (\text{B5})$$

respectively. By multiplying Eq. (B5) by P and taking the trace, we can also have

$$\sum_\mu \sigma_\mu (1 - \cos \phi) \text{Tr}(P \nabla_\mu^2 P) + \sum_\mu \sigma_\mu \sin \phi \nabla_\mu \phi \text{Tr}(P \nabla_\mu P) = 0. \quad (\text{B6})$$

As $\text{Tr}(P \nabla_\nu P) = 0$, and $\text{Tr}(P \nabla_\nu^2 P) = \nabla_\nu \text{Tr}(P \nabla_\nu P) - \text{Tr}(\nabla_\nu P)^2 = -\text{Tr}(\nabla_\nu P)^2$, Eq. (B6) means either $\sum_\mu \sigma_\mu \text{Tr}(\nabla_\mu P)^2 = 0$ or $\phi = 2\pi\mathbb{Z}$. For $\phi = 2\pi\mathbb{Z}$, Q in Eq. (5) becomes independent of $P(\mathbf{r})$, where we can choose $P(\mathbf{r})$ freely. Note that $P(\mathbf{r})$ that satisfies $\sum_\mu \sigma_\mu \text{Tr}(\nabla_\mu P)^2 = 0$ becomes independent of r ; $P(\mathbf{r}) = P_0$. This is because as $\sigma_\mu \geq 0$, $\sum_\mu \sigma_\mu \text{Tr}(\nabla_\mu P)^2 = \sum_\mu \sum_{i,j=1}^N \sigma_\mu |\nabla_\mu P_{ij}(\mathbf{r})|^2 = 0$ requires that $P(\mathbf{r})$ is independent of \mathbf{r} . For $\phi = 2\pi\mathbb{Z}$, we choose $P(\mathbf{r}) = P_0$, so that $\sum_\mu \sigma_\mu \text{Tr}(\nabla_\mu P)^2 = 0$ is satisfied entirely. Then, Eq. (B4) reduces to a Poisson equation,

$$(\sigma_\mu + c_\mu) \nabla_\mu^2 \phi = 0. \quad (\text{B7})$$

Note also that when ϕ is indefinite such as in vortex cores, Eqs. (B5,B6) do not have to be satisfied, where $P(\mathbf{r})$ is not specified: $P(\mathbf{r})$ can depend on r along vortex loops. From Eq. (B2), the field strength $F_\mu \equiv \epsilon_{\mu\nu\lambda} \nabla_\nu h_\lambda + i\epsilon_{\mu\nu\lambda} h_\nu h_\lambda$ with $h_\lambda \equiv -iQ^{-1} \nabla_\lambda Q$ can be calculated,

$$F_\mu(\mathbf{r}) \equiv \epsilon_{\mu\nu\lambda} \nabla_\nu \nabla_\mu \phi(\mathbf{r}) P(\mathbf{r}). \quad (\text{B8})$$

Appendix C: Variational study of $U(N)$ type-II superconductor model

In this Appendix, we elaborate the variational analysis of the superconducting (Meissner) phase in the $U(N)$ type-II superconductor model for $\chi = 0$ case, Eqs. (35,36,37,38). In the superconducting phase, the ψ field assumes a spatially uniform value, and the spin-wave fluctuation around the uniform configuration can be absorbed into the $U(1)$ gauge field. The action thus obtained takes the following form in the continuum limit,

$$S = 2\pi \int d^3r \left[\frac{(\nabla \times \boldsymbol{\theta}^0)^2}{\sigma + Nc} + \sum_a \frac{(\nabla \times \boldsymbol{\theta}^a)^2}{\sigma} \right] - 2t \sum_\mu \int d^3r \int d|p(\mathbf{r})\rangle \cos \text{Tr}(2\pi\Theta_\mu P). \quad (\text{C1})$$

Thanks to the $|p(\mathbf{r})\rangle$ integral, the $U(1)$ and $SU(N)$ gauge fields are decoupled from one another at the quadratic level in the Taylor expansion of the cos term. Thus, the Meissner phase can be described by the following mean-field action with finite m ,

$$\bar{S} = 2\pi \int d^3r \left\{ \left[\frac{(\nabla \times \boldsymbol{\theta}^0)^2}{\sigma + Nc} + m^2 (\boldsymbol{\theta}^0)^2 \right] + \sum_{a=1}^{N^2-1} \left[\frac{(\nabla \times \boldsymbol{\theta}^a)^2}{\sigma} + m^2 (\boldsymbol{\theta}^a)^2 \right] \right\}. \quad (\text{C2})$$

Here we assume the same mass m for the $U(1)$ and $SU(N)$ gauge field (see the replica limit of Eq. (46)). To obtain a gap equation for m , we exercise a variational principle which states that a trial free energy $F(m)$ defined below must be always greater than the true free energy $F_{\text{true}} \equiv -\ln Z \equiv \int D[\Theta] \exp[-S]$,

$$F(m) \equiv -\ln \bar{Z} + \langle S - \bar{S} \rangle_{\bar{S}}, \quad (\text{C3})$$

and

$$\begin{aligned} \langle \cdots \rangle_{\bar{S}} &\equiv \frac{1}{\bar{Z}} \int D[\Theta] \cdots \exp[-\bar{S}], \\ \bar{Z} &\equiv \int D[\Theta] \exp[-\bar{S}]. \end{aligned} \quad (\text{C4})$$

The variational principle (Bogoliubov inequality) is rooted in the convex nature of the exponential function, which implies that an optimal value of m can be obtained by minimizing $F(m)$ with respect to m [2, 124, 128].

Notably, $F(m)$ reaches zero in the replica limit[see below], and so does F_{true} by the inequality. Since $F_{\text{true}} = -\ln \langle \mathcal{Z}^N \rangle_{\text{dis}}$ in Eq. (1), $\lim_{N \rightarrow 0} F_{\text{true}} = 0$ allows us to express the disorder-averaged free energy by $-\langle \ln \mathcal{Z} \rangle_{\text{dis}} = \lim_{N \rightarrow 0} F_{\text{true}}/N$. Correspondingly, we regard $\lim_{N \rightarrow 0} F(m)/N$ as a trial function of the disorder-averaged free energy and minimize this trial function with respect to m . The following Green's functions, as well as their trace and determinant, facilitate an evaluation of $F(m)$,

$$\begin{aligned} G_{\mu\nu}^a(\mathbf{r} - \mathbf{r}') &\equiv \int \frac{d^3k}{(2\pi)^3} \langle \tilde{\theta}_\mu^a(-\mathbf{k}) \tilde{\theta}_\nu^a(\mathbf{k}) \rangle_{\bar{S}} e^{i\mathbf{k} \cdot (\mathbf{r} - \mathbf{r}')} \\ &\equiv \int \frac{d^3k}{(2\pi)^3} \tilde{G}_{\mu\nu}^a(\mathbf{k}) e^{i\mathbf{k} \cdot (\mathbf{r} - \mathbf{r}')} \end{aligned} \quad (\text{C5})$$

with $a = 0, 1, \dots, N^2 - 1$. The Fourier transforms $\tilde{G}_{\mu\nu}^a(\mathbf{k})$ of the Green's function are given by

$$\tilde{G}_{\mu\nu}^0(\mathbf{k}) = \frac{1}{4\pi} \frac{1}{k^2 + (\sigma + Nc)m^2} \left[(\sigma + Nc)\delta_{\mu\nu} + \frac{k_\mu k_\nu}{m^2} \right], \quad (\text{C6})$$

$$\tilde{G}_{\mu\nu}^{a \neq 0}(\mathbf{k}) = \frac{1}{4\pi} \frac{1}{k^2 + \sigma m^2} \left(\sigma \delta_{\mu\nu} + \frac{k_\mu k_\nu}{m^2} \right). \quad (\text{C7})$$

The trace and determinant of these 3 by 3 matrices are as follows, e.g.

$$\begin{aligned} \text{Tr} \tilde{G}^{a \neq 0}(\mathbf{k}) &= \frac{1}{4\pi} \frac{k^2 + 3\sigma m^2}{m^2(k^2 + \sigma m^2)}, \\ \det \tilde{G}^{a \neq 0}(\mathbf{k}) &= \frac{\sigma^2}{64\pi^3} \frac{1}{m^2(k^2 + \sigma m^2)^2}. \end{aligned} \quad (\text{C8})$$

We calculate the density of the trial free energy $F(m)$ in the replica limit,

$$f(m) = \lim_{N \rightarrow 0} \frac{F(m)}{NV} = - \lim_{N \rightarrow 0} \frac{\ln \bar{Z}}{NV} + \lim_{N \rightarrow 0} \frac{\langle S - \bar{S} \rangle_{\bar{S}}}{NV} \quad (\text{C9})$$

where the m -dependent part of $\ln \bar{Z}/V$ is given by the determinant of the Green's function,

$$\begin{aligned} \frac{1}{V} \ln \bar{Z} &= \frac{1}{2} \sum_{a=0}^{N^2-1} \int \frac{d^3 k}{(2\pi)^3} \ln \det \tilde{G}^a(\mathbf{k}) \\ &= - \int \frac{d^3 k}{(2\pi)^3} \ln \frac{k^2 + (\sigma + Nc)m^2}{k^2 + \sigma m^2} - N^2 \int \frac{d^3 k}{(2\pi)^3} [\ln m + \ln(k^2 + \sigma m^2)], \end{aligned} \quad (\text{C10})$$

In the replica limit, it becomes

$$\begin{aligned} \lim_{N \rightarrow 0} \frac{1}{NV} \ln \bar{Z} &= - \lim_{N \rightarrow 0} \frac{2}{N} \int \frac{d^3 k}{(2\pi)^3} \ln \frac{k^2 + (\sigma + Nc)m^2}{k^2 + \sigma m^2} \\ &= - \int \frac{d^3 k}{(2\pi)^3} \frac{2cm^2}{k^2 + \sigma m^2}. \end{aligned} \quad (\text{C11})$$

$\langle S - \bar{S} \rangle_{\bar{S}}$ is given by

$$\langle S - S_0 \rangle_{\bar{S}} = -2t \sum_{\mu} \int d^3 r \int d|p(\mathbf{r})| \langle \cos \text{Tr}(2\pi \Theta_{\mu} P) \rangle_{\bar{S}} - 2\pi m^2 \sum_{a=0}^{N^2-1} \sum_{\mu=x,y,z} \int d^3 r \langle \theta_{\mu}^a(\mathbf{r}) \theta_{\mu}^a(\mathbf{r}) \rangle_{\bar{S}}, \quad (\text{C12})$$

where

$$\sum_{\mu} \langle \theta_{\mu}^0(\mathbf{r}) \theta_{\mu}^0(\mathbf{r}) \rangle_{\bar{S}} = \int \frac{d^3 k}{(2\pi)^3} \text{Tr} \tilde{G}^0(\mathbf{k}) = \frac{1}{4\pi} \int \frac{d^3 k}{(2\pi)^3} \frac{k^2 + 3(\sigma + Nc)m^2}{m^2[k^2 + (\sigma + Nc)m^2]}, \quad (\text{C13})$$

$$\sum_{\mu} \langle \theta_{\mu}^{a \neq 0}(\mathbf{r}) \theta_{\mu}^{a \neq 0}(\mathbf{r}) \rangle_{\bar{S}} = \int \frac{d^3 k}{(2\pi)^3} \text{Tr} \tilde{G}^{a \neq 0}(\mathbf{k}) = \frac{1}{4\pi} \int \frac{d^3 k}{(2\pi)^3} \frac{k^2 + 3\sigma m^2}{m^2(k^2 + \sigma m^2)}. \quad (\text{C14})$$

The first term in Eq. (C12) for general N is given by

$$\langle \cos \text{Tr}(2\pi \Theta_{\mu}(\mathbf{r}) P) \rangle_{\bar{S}} = \left\langle \cos \left[2\pi \frac{\theta_{\mu}^0(\mathbf{r})}{\sqrt{N}} + 2\pi \sum_{a=1}^{N^2-1} \theta_{\mu}^a(\mathbf{r}) \text{Tr}(T^a P) \right] \right\rangle \quad (\text{C15})$$

$$= \exp \left[-\frac{2\pi^2}{N} \int \frac{d^3 k}{(2\pi)^3} \tilde{G}_{\mu\mu}^0(\mathbf{k}) - 2\pi^2 \sum_{a=1}^{N^2-1} \text{Tr}^2(T^a P) \int \frac{d^3 k}{(2\pi)^3} \tilde{G}_{\mu\mu}^a(\mathbf{k}) \right]. \quad (\text{C16})$$

Using

$$\sum_{a=1}^{N^2-1} \text{Tr}^2(T^a P) = \sum_{a=1}^{N^2-1} T_{ij}^a P_{ji} T_{kl}^a P_{lk} = \left(\delta_{il} \delta_{jk} - \frac{1}{N} \delta_{ij} \delta_{kl} \right) P_{ji} P_{lk} = \text{Tr} P^2 - \frac{1}{N} \text{Tr}^2 P = 1 - \frac{1}{N}, \quad (\text{C17})$$

we can express this by

$$\langle \cos \text{Tr}(2\pi \Theta_{\mu}(\mathbf{r}) P) \rangle_{\bar{S}} = \exp \left\{ -2\pi^2 \int \frac{d^3 k}{(2\pi)^3} \left[\frac{1}{N} \tilde{G}_{\mu\mu}^0(\mathbf{k}) + \left(1 - \frac{1}{N} \right) \tilde{G}_{\mu\mu}^{a \neq 0}(\mathbf{k}) \right] \right\}. \quad (\text{C18})$$

For a spherical integral region of k (the region will be specified later), we can also rewrite this by

$$\langle \cos \text{Tr}(2\pi \Theta_{\mu}(\mathbf{r}) P) \rangle_{\bar{S}} = \exp \left\{ -\frac{2\pi^2}{3} \int \frac{d^3 k}{(2\pi)^3} \left[\frac{1}{N} \text{Tr} \tilde{G}^0(\mathbf{k}) + \left(1 - \frac{1}{N} \right) \text{Tr} \tilde{G}^{a \neq 0}(\mathbf{k}) \right] \right\}. \quad (\text{C19})$$

In the limit of $N \rightarrow 0$, the integrand of Eq. (C19) remains a finite function of k

$$\lim_{N \rightarrow 0} \left[\frac{1}{N} \text{Tr} \tilde{G}^0(\mathbf{k}) + \left(1 - \frac{1}{N}\right) \text{Tr} \tilde{G}^{a \neq 0}(\mathbf{k}) \right] = \frac{1}{4\pi} \frac{k^4 + 2(2\sigma + c)m^2k^2 + 3\sigma^2m^4}{m^2(k^2 + \sigma m^2)^2}. \quad (\text{C20})$$

The second term of Eq. (C12) for general N is given by

$$\frac{2\pi m^2}{V} \int d^3r \sum_{a=0}^{N^2-1} \langle [\theta^a(\mathbf{r})]^2 \rangle_{\bar{S}} = \frac{1}{2} \int \frac{d^3k}{(2\pi)^3} \left[\frac{k^2 + 3(\sigma + Nc)m^2}{k^2 + (\sigma + Nc)m^2} - \frac{k^2 + 3\sigma m^2}{k^2 + \sigma m^2} \right] + \frac{N^2}{2} \int \frac{d^3k}{(2\pi)^3} \frac{k^2 + 3\sigma m^2}{k^2 + \sigma m^2}. \quad (\text{C21})$$

which vanishes in the replica limit. Thus, we obtain

$$\lim_{N \rightarrow 0} \frac{2\pi m^2}{NV} \int d^3r \sum_{a=0}^{N^2-1} \langle (\theta^a(\mathbf{r}))^2 \rangle_{\bar{S}} = \int \frac{d^3k}{(2\pi)^3} \frac{cm^2k^2}{(k^2 + \sigma m^2)^2}. \quad (\text{C22})$$

To summarize, we obtain $F(m)/V$ for general N as follows,

$$\frac{F(m)}{V} = -\frac{6t\pi^{N-1}}{\Gamma(N)} \exp \left\{ -\frac{2\pi^2}{3} \int \frac{d^3k}{(2\pi)^3} \left[\frac{1}{N} \text{Tr} \tilde{G}^0(\mathbf{k}) + \left(1 - \frac{1}{N}\right) \text{Tr} \tilde{G}^a(\mathbf{k}) \right] \right\} \quad (\text{C23})$$

$$- \frac{1}{2} \int \frac{d^3k}{(2\pi)^3} \left[\frac{k^2 + 3(\sigma + Nc)m^2}{k^2 + (\sigma + Nc)m^2} - \frac{k^2 + 3\sigma m^2}{k^2 + \sigma m^2} \right] - \frac{N^2}{2} \int \frac{d^3k}{(2\pi)^3} \frac{k^2 + 3\sigma m^2}{k^2 + \sigma m^2} \quad (\text{C24})$$

$$+ \int \frac{d^3k}{(2\pi)^3} \ln \frac{k^2 + (\sigma + Nc)m^2}{k^2 + \sigma m^2} + N^2 \int \frac{d^3k}{(2\pi)^3} [\ln m + \ln(k^2 + \sigma m^2)], \quad (\text{C25})$$

where we use $\int d|p(\mathbf{r})\rangle = \pi^{N-1}/\Gamma(N)$. This quantity vanishes linearly in N in the replica limit with

$$f(m) \equiv \lim_{N \rightarrow 0} \frac{F(m)}{NV} = -\frac{6y}{\pi} \exp \left[-\frac{\pi}{6} \int \frac{d^3k}{(2\pi)^3} \frac{k^4 + 2(2\sigma + c)m^2k^2 + 3\sigma^2m^4}{m^2(k^2 + \sigma m^2)^2} \right] \\ - \int \frac{d^3k}{(2\pi)^3} \frac{cm^2k^2}{(k^2 + \sigma m^2)^2} + \int \frac{d^3k}{(2\pi)^3} \frac{cm^2}{k^2 + \sigma m^2}. \quad (\text{C26})$$

Note that all three k -integrals on the right-hand side need the ultraviolet (UV) cutoff. Here, we use the following soft-cutoff function,

$$\Psi(\mathbf{k}) = \frac{\Lambda^4}{(k^2 + \Lambda^2)^2}, \quad (\text{C27})$$

and replace the k -integrals by integrals with the cutoff function, i.e.

$$\int \frac{d^3k}{(2\pi)^3} \cdots \rightarrow \int \frac{d^3k}{(2\pi)^3} \Psi(\mathbf{k}) \cdots \quad (\text{C28})$$

The k -integrals are calculated as follows,

$$\int \frac{d^3k}{(2\pi)^3} \frac{\Lambda^4}{(k^2 + \Lambda^2)^2} \frac{k^4 + 2(2\sigma + c)m^2k^2 + 3\sigma^2m^4}{m^2(k^2 + \sigma m^2)^2} \\ = \frac{\Lambda^3 \Lambda^3 + |m| [3\sqrt{\sigma}\Lambda^2 + |m| (2c\Lambda + 5\sigma\Lambda + 3m\sigma^{3/2})]}{8\pi m^2 (\Lambda + \sqrt{\sigma}|m|)^3}, \quad (\text{C29})$$

$$\int \frac{d^3k}{(2\pi)^3} \frac{\Lambda^4}{(k^2 + \Lambda^2)^2} \frac{cm^2k^2}{(k^2 + \sigma m^2)^2} = \frac{1}{8\pi} \frac{cm^2\Lambda^4}{(\Lambda + m\sqrt{\sigma})^3}, \quad (\text{C30})$$

$$\int \frac{d^3k}{(2\pi)^3} \frac{\Lambda^4}{(k^2 + \Lambda^2)^2} \frac{cm^2}{k^2 + \sigma m^2} = \frac{1}{8\pi} \frac{cm^2\Lambda^3}{(\Lambda + m\sqrt{\sigma})^2}. \quad (\text{C31})$$

Thus, we finally obtain,

$$f = -\frac{6t}{\pi} \exp \left\{ -\frac{\Lambda^3 \Lambda^3 + |m| [3\sqrt{\sigma}\Lambda^2 + |m| (2c\Lambda + 5\sigma\Lambda + 3m\sigma^{3/2})]}{48 m^2 (\Lambda + \sqrt{\sigma}|m|)^3} \right\} + \frac{1}{8\pi} \frac{c\sqrt{\sigma}m^3\Lambda^3}{(\Lambda + m\sqrt{\sigma})^3}. \quad (\text{C32})$$

-
- [1] N. D. Mermin. The topological theory of defects in ordered media. *Rev. Mod. Phys.*, 51:591–648, Jul 1979.
- [2] P. M. Chaikin and T. C. Lubensky. *Principles of condensed matter physics*. Cambridge University Press, 1995.
- [3] Charles Kittel. Theory of the structure of ferromagnetic domains in films and small particles. *Phys. Rev.*, 70:965–971, Dec 1946.
- [4] James P. Sethna. *Statistical Mechanics: Entropy, Order Parameters, and Complexity*. Oxford University Press, 2006.
- [5] Lars Onsager. Statistical hydrodynamics. *Nuovo Cimento (Supplemento)*, 6:279–287, 1949.
- [6] Richard P. Feynman. Application of quantum mechanics to liquid helium. *Progress in Low Temperature Physics*, 1:17–53, 1955.
- [7] Alexei Abrikosov. On the magnetic properties of superconductors of the second group. *Soviet Physics JETP*, 5:1174–1182, 1957.
- [8] Michael Tinkham. *Introduction to Superconductivity*. McGraw-Hill, 1996.
- [9] Russell J. Donnelly. *Quantized Vortices in Helium II*. Cambridge University Press, 1991.
- [10] T. H. R. Skyrme and Basil Ferdinand Jamieson Schonland. A non-linear field theory. *Proceedings of the Royal Society of London. Series A. Mathematical and Physical Sciences*, 260(1300):127–138, 1961.
- [11] T.H.R. Skyrme. A unified field theory of mesons and baryons. *Nuclear Physics*, 31:556–569, 1962.
- [12] A. N. Bogdanov and D. A. Yablonskii. Thermodynamically stable 'vortices' in magnetically ordered crystals. the mixed state of magnets." *Soviet Physics - JETP*, 68:101, 1989.
- [13] N. Nagaosa and Y. Tokura. Topological properties of dynamics of magnetic skyrmions. *Nature Nanotechnology*, 8:899, 2013.
- [14] A. Fert, N. Reyren, and V. Cros. Magnetic skyrmions: advances in physics and potential applications. *Nat. Rev. Mater.*, 2:17031, 2017.
- [15] V L Berezinskii. Destruction of long-range order in one-dimensional and two-dimensional systems having a continuous symmetry group i. classical systems. *Soviet Journal of Experimental and Theoretical Physics*, 32(3):493, 1971.
- [16] V L Berezinskii. Destruction of long-range order in one-dimensional and two-dimensional systems having a continuous symmetry group ii. classical systems. *Soviet Journal of Experimental and Theoretical Physics*, 34(3):610, 1972.
- [17] J M Kosterlitz and D J Thouless. Ordering, metastability and phase transitions in two-dimensional systems. *Journal of Physics C: Solid State Physics*, 6(7):1181, apr 1973.
- [18] J M Kosterlitz. The critical properties of the two-dimensional xy model. *Journal of Physics C: Solid State Physics*, 7(6):1046, mar 1974.
- [19] David R. Nelson and B. I. Halperin. Dislocation-mediated melting in two dimensions. *Phys. Rev. B*, 19:2457–2484, Mar 1979.
- [20] A. P. Young. Melting and the vector coulomb gas in two dimensions. *Phys. Rev. B*, 19:1855–1866, Feb 1979.
- [21] B. I. Halperin and David R. Nelson. Theory of two-dimensional melting. *Phys. Rev. Lett.*, 41:121–124, Jul 1978.
- [22] David R. Nelson and Daniel S. Fisher. Dynamics of classical XY spins in one and two dimensions. *Phys. Rev. B*, 16:4945–4955, Dec 1977.
- [23] C. Dasgupta and B. I. Halperin. Phase transition in a lattice model of superconductivity. *Phys. Rev. Lett.*, 47:1556–1560, Nov 1981.
- [24] Gary A. Williams. Vortex-ring model of the superfluid λ transition. *Phys. Rev. Lett.*, 59:1926–1929, Oct 1987.
- [25] Subodh R. Shenoy. Vortex-loop scaling in the three-dimensional xy ferromagnet. *Phys. Rev. B*, 40:5056–5068, Sep 1989.
- [26] T W B Kibble. Topology of cosmic domains and strings. *Journal of Physics A: Mathematical and General*, 9(8):1387, aug 1976.
- [27] W. H. Zurek. Cosmological experiments in superfluid helium ? *Nature*, 317:505–508, 1985.
- [28] W. H. Zurek. Cosmological experiments in condensed matter systems. *Physics Reports*, 276:177–221, 1996.
- [29] P. W. Anderson. Absence of diffusion in certain random lattices. *Phys. Rev.*, 109:1492–1505, Mar 1958.
- [30] D.J. Thouless. Electrons in disordered systems and the theory of localization. *Physics Reports*, 13(3):93–142, 1974.
- [31] E. Abrahams, P. W. Anderson, D. C. Licciardello, and T. V. Ramakrishnan. Scaling theory of localization: Absence of quantum diffusion in two dimensions. *Phys. Rev. Lett.*, 42:673–676, Mar 1979.
- [32] T. F. Rosenbaum, K. Andres, G. A. Thomas, and R. N. Bhatt. Sharp metal-insulator transition in a random solid. *Phys. Rev. Lett.*, 45:1723–1726, Nov 1980.
- [33] D. C. Tsui, H. L. Stormer, and A. C. Gossard. Two-dimensional magnetotransport in the extreme quantum limit. *Phys. Rev. Lett.*, 48:1559–1562, May 1982.
- [34] J. Wang and A. Genack. Transport through modes in random media. *Nature*, 471:345–348, 2011.
- [35] H. Hu, A. Strybulevych, J. H. Page, S. E. Skipetrov, and van Tiggelen B. A. Localization of ultrasound in a three-dimensional elastic network. *Nature Physics*, 4:945–948, 2008.
- [36] G. Roati, C. D'Errico, C. Fallani, M. Fattori, C. Fort, M. Zaccanti, G. Modugno, M. Modugno, and M. Inguscio. Anderson localization of a non-interacting bose-einstein condensate. *Nature*, 453:895–898, 2008.
- [37] S E Skipetrov and J H Page. Red light for anderson localization. *New Journal of Physics*, 18(2):021001, jan 2016.
- [38] F. J. Wegner. lectrons in disordered systems. scaling near the mobility edge. *Z. Physik B Condensed Matter*, 25:327–2337, 1976.
- [39] F. Wegner. The mobility edge problem: Continuous symmetry and a conjecture. *Z. Physik B Condensed Matter*, 35:207–210, 1979.
- [40] K. B. Efetov, A. I. Larkin, and D. E. Khmel'nitskii. Interaction of diffusion modes in the theory of localization. *Sov. Phys. JETP*, 52:568, 1980.
- [41] Shinobu Hikami, Anatoly I. Larkin, and Yosuke Nagaoka. Spin-orbit interaction and magnetoresistance in the two dimensional random system. *Progress of Theoretical*

- Physics*, 63(2):707–710, 02 1980.
- [42] Shinobu Hikami. Anderson localization in a nonlinear- σ -model representation. *Phys. Rev. B*, 24:2671–2679, Sep 1981.
- [43] K. B. Efetov. Supersymmetry and theory of disordered metals. *Advances in Physics*, 32(1):53–127, 1983.
- [44] A. MacKinnon and B. Kramer. One-parameter scaling of localization length and conductance in disordered systems. *Phys. Rev. Lett.*, 47:1546–1549, Nov 1981.
- [45] A. MacKinnon and B. Kramer. The scaling theory of electrons in disordered solids: Additional numerical results. *Z. Physik B Condensed Matter*, 53:1–13, 1983.
- [46] Alexander Altland and Martin R. Zirnbauer. Non-standard symmetry classes in mesoscopic normal-superconducting hybrid structures. *Physical Review B*, 55(2):1142–1161, 1997.
- [47] Keith Slevin and Tomi Ohtsuki. Corrections to scaling at the anderson transition. *Phys. Rev. Lett.*, 82:382–385, Jan 1999.
- [48] Ferdinand Evers and Alexander D. Mirlin. Anderson transitions. *Reviews of Modern Physics*, 80(4):1355–1417, 2008.
- [49] Keith Slevin and Tomi Ohtsuki. Critical exponent for the Anderson transition in the three-dimensional orthogonal universality class. *New Journal of Physics*, 16(1):015012, 2014.
- [50] Kohei Kawabata, Ken Shiozaki, Masahito Ueda, and Masatoshi Sato. Symmetry and Topology in Non-Hermitian Physics. *Physical Review X*, 9(4):041015, 2019.
- [51] D. Bernard and A. LeClair. A Classification of Non-Hermitian Random Matrices. In A. Cappelli and G. Musardo, editors, *Statistical Field Theories*, volume 73 of *NATO Science Series*, pages 207–214, 2002.
- [52] Hengyun Zhou and Jong Yeon Lee. Periodic table for topological bands with non-hermitian symmetries. *Phys. Rev. B*, 99:235112, Jun 2019.
- [53] Kohei Kawabata and Shinsei Ryu. Nonunitary scaling theory of non-hermitian localization. *Phys. Rev. Lett.*, 126:166801, Apr 2021.
- [54] Xunlong Luo, Zhenyu Xiao, Kohei Kawabata, Tomi Ohtsuki, and Ryuichi Shindou. Unifying the Anderson transitions in Hermitian and non-Hermitian systems. *Physical Review Research*, 4(2):L022035, 2022.
- [55] Ze Chen, Kohei Kawabata, Anish Kulkarni, and Shinsei Ryu. Field theory of non-hermitian disordered systems. *Phys. Rev. B*, 111:054203, Feb 2025.
- [56] Naomichi Hatano and David R. Nelson. Localization transitions in non-hermitian quantum mechanics. *Phys. Rev. Lett.*, 77:570–573, Jul 1996.
- [57] H. Cao, Y. G. Zhao, S. T. Ho, E. W. Seelig, Q. H. Wang, and R. P. H. Chang. Random laser action in semiconductor powder. *Phys. Rev. Lett.*, 82:2278–2281, Mar 1999.
- [58] D. Wiersma. The physics and applications of random lasers. *Nature Physics*, 4:359–367, 2008.
- [59] D. Wiersma. Disordered photonics. *Nature Photonics*, 7:188–196, 2013.
- [60] Alexey G. Yamilov, Raktim Sarma, Brandon Redding, Ben Payne, Heeso Noh, and Hui Cao. Position-dependent diffusion of light in disordered waveguides. *Phys. Rev. Lett.*, 112:023904, Jan 2014.
- [61] A. Basiri, Y. Bromberg, A. Yamilov, H. Cao, and T. Kottos. Light localization induced by a random imaginary refractive index. *Phys. Rev. A*, 90:043815, Oct 2014.
- [62] Baolong Xu, Tomi Ohtsuki, and Ryuichi Shindou. Integer quantum magnon hall plateau-plateau transition in a spin-ice model. *Phys. Rev. B*, 94:220403, Dec 2016.
- [63] I. Yusipov, T. Lapyteva, S. Denisov, and M. Ivanchenko. Localization in open quantum systems. *Phys. Rev. Lett.*, 118:070402, Feb 2017.
- [64] Ryusuke Hamazaki, Kohei Kawabata, and Masahito Ueda. Non-hermitian many-body localization. *Phys. Rev. Lett.*, 123:090603, Aug 2019.
- [65] A. F. Tzortzakakis, K. G. Makris, and E. N. Economou. Non-hermitian disorder in two-dimensional optical lattices. *Phys. Rev. B*, 101:014202, Jan 2020.
- [66] C. Wang and X. R. Wang. Level statistics of extended states in random non-hermitian hamiltonians. *Phys. Rev. B*, 101:165114, Apr 2020.
- [67] Yi Huang and B. I. Shklovskii. Anderson transition in three-dimensional systems with non-hermitian disorder. *Phys. Rev. B*, 101:014204, Jan 2020.
- [68] Yi Huang and B. I. Shklovskii. Spectral rigidity of non-hermitian symmetric random matrices near the anderson transition. *Phys. Rev. B*, 102:064212, Aug 2020.
- [69] S. Weidemann, M. Kremer, S. Longhi, and A. Szameit. Coexistence of dynamical delocalization and spectral localization through stochastic dissipation. *Nature Photonics*, 15:576–581, 2021.
- [70] Jahan Claes and Taylor L. Hughes. Skin effect and winding number in disordered non-hermitian systems. *Phys. Rev. B*, 103:L140201, Apr 2021.
- [71] Yanxia Liu, Qi Zhou, and Shu Chen. Localization transition, spectrum structure, and winding numbers for one-dimensional non-hermitian quasicrystals. *Phys. Rev. B*, 104:024201, Jul 2021.
- [72] Hui Liu, Jih-Shih You, Shinsei Ryu, and Ion Cosma Fulga. Supermetal-insulator transition in a non-hermitian network model. *Phys. Rev. B*, 104:155412, Oct 2021.
- [73] Xunlong Luo, Tomi Ohtsuki, and Ryuichi Shindou. Universality classes of the anderson transitions driven by non-hermitian disorder. *Phys. Rev. Lett.*, 126:090402, Mar 2021.
- [74] Xunlong Luo, Tomi Ohtsuki, and Ryuichi Shindou. Transfer matrix study of the Anderson transition in non-Hermitian systems. *Physical Review B*, 104(10):104203, 2021.
- [75] Giuseppe De Tomasi and Ivan M. Khaymovich. Non-hermiticity induces localization: Good and bad resonances in power-law random banded matrices. *Phys. Rev. B*, 108:L180202, Nov 2023.
- [76] C. Wang and X. R. Wang. Anderson localization transitions in disordered non-hermitian systems with exceptional points. *Phys. Rev. B*, 107:024202, Jan 2023.
- [77] Yin-Quan Huang, Yu-Min Hu, Wen-Tan Xue, and Zhong Wang. Universal scaling of green’s functions in disordered non-hermitian systems. *Phys. Rev. B*, 111:L060203, Feb 2025.
- [78] Liang-Hong Mo, Zhenyu Xiao, Roderich Moessner, and Hongzheng Zhao. Non-hermitian delocalization in 1d via emergent compactness, 2025.
- [79] Renate Gade and Franz Wegner. The $n = 0$ replica limit of $U(n)$ and $U(n)SO(n)$ models. *Nuclear Physics B*, 360(2):213–218, 1991.
- [80] Renate Gade. Anderson localization for sublattice models. *Nuclear Physics B*, 398(3):499–515, 1993.

- [81] Leon Balents and Matthew P. A. Fisher. Delocalization transition via supersymmetry in one dimension. *Physical Review B*, 56(20):12970–12991, 1997.
- [82] Yasuhiro Hatsugai, Xiao-Gang Wen, and Mahito Kohmoto. Disordered critical wave functions in random-bond models in two dimensions: Random-lattice fermions at $e = 0$ without doubling. *Phys. Rev. B*, 56:1061–1064, Jul 1997.
- [83] Alexander Altland and B.D. Simons. Field theory of the random flux model. *Nuclear Physics B*, 562(3):445–476, 1999.
- [84] Takahiro Fukui. Critical behavior of two-dimensional random hopping fermions with π -flux. *Nuclear Physics B*, 562(3):477–496, 1999.
- [85] Michele Fabrizio and Claudio Castellani. Anderson localization in bipartite lattices. *Nuclear Physics B*, 583(3):542–583, 2000.
- [86] S. Guruswamy, A. LeClair, and A.W.W. Ludwig. $gl(n-n)$ super-current algebras for disordered dirac fermions in two dimensions. *Nuclear Physics B*, 583(3):475–512, 2000.
- [87] Olexei Motrunich, Kedar Damle, and David A. Huse. Particle-hole symmetric localization in two dimensions. *Phys. Rev. B*, 65:064206, Jan 2002.
- [88] Baruch Horovitz and Pierre Le Doussal. Freezing transitions and the density of states of two-dimensional random dirac hamiltonians. *Phys. Rev. B*, 65:125323, Mar 2002.
- [89] C. Mudry, S. Ryu, and A. Furusaki. Density of states for the π -flux state with bipartite real random hopping only: A weak disorder approach. *Phys. Rev. B*, 67:064202, Feb 2003.
- [90] Marc Bocquet and J. T. Chalker. Network models for localization problems belonging to the chiral symmetry classes. *Phys. Rev. B*, 67:054204, Feb 2003.
- [91] Hiroki Yamada and Takahiro Fukui. Random hopping fermions on bipartite lattices: density of states, inverse participation ratios, and their correlations in a strong disorder regime. *Nuclear Physics B*, 679(3):632–646, 2004.
- [92] Antonio M. García-García and Emilio Cuevas. Anderson transition in systems with chiral symmetry. *Phys. Rev. B*, 74:113101, Sep 2006.
- [93] Luca Dell’Anna. Anomalous dimensions of operators without derivatives in the non-linear σ -model for disordered bipartite lattices. *Nuclear Physics B*, 750(3):213–228, 2006.
- [94] P. Markoš and L. Schweitzer. Critical conductance of two-dimensional chiral systems with random magnetic flux. *Phys. Rev. B*, 76:115318, Sep 2007.
- [95] E. J. König, P. M. Ostrovsky, I. V. Protopopov, and A. D. Mirlin. Metal-insulator transition in two-dimensional random fermion systems of chiral symmetry classes. *Physical Review B*, 85(19):195130, 2012.
- [96] Ian Mondragon-Shem, Taylor L. Hughes, Juntao Song, and Emil Prodan. Topological criticality in the chiral-symmetric aiii class at strong disorder. *Phys. Rev. Lett.*, 113:046802, Jul 2014.
- [97] Xunlong Luo, Baolong Xu, Tomi Ohtsuki, and Ryuichi Shindou. Critical behavior of Anderson transitions in three-dimensional orthogonal classes with particle-hole symmetries. *Physical Review B*, 101(2):020202, 2020.
- [98] Chang-An Li, Bo Fu, Zi-Ang Hu, Jian Li, and Shun-Qing Shen. Topological phase transitions in disordered electric quadrupole insulators. *Phys. Rev. Lett.*, 125:166801, Oct 2020.
- [99] Tong Wang, Tomi Ohtsuki, and Ryuichi Shindou. Universality classes of the anderson transition in the three-dimensional symmetry classes aiii, bdi, c, d, and ci. *Phys. Rev. B*, 104:014206, Jul 2021.
- [100] Jonas F. Karcher, Ilya A. Gruzberg, and Alexander D. Mirlin. Metal-insulator transition in a two-dimensional system of chiral unitary class. *Physical Review B*, 107(2):L020201, 2023.
- [101] Jonas F. Karcher, Ilya A. Gruzberg, and Alexander D. Mirlin. Generalized multifractality in two-dimensional disordered systems of chiral symmetry classes. *Phys. Rev. B*, 107:104202, Mar 2023.
- [102] Zhenyu Xiao, Kohei Kawabata, Xunlong Luo, Tomi Ohtsuki, and Ryuichi Shindou. Anisotropic Topological Anderson Transitions in Chiral Symmetry Classes. *Physical Review Letters*, 131(5):056301, 2023.
- [103] Pengwei Zhao, Zhenyu Xiao, Yeyang Zhang, and Ryuichi Shindou. Topological Effect on the Anderson Transition in Chiral Symmetry Classes. *Physical Review Letters*, 133(22):226601, 2024.
- [104] João S. Silva, Miguel Gonçalves, Eduardo V. Castro, Pedro Ribeiro, and Miguel A. N. Araújo. Disorder-induced instability of a weyl nodal loop semimetal towards a diffusive topological metal with protected multifractal surface states. *Phys. Rev. B*, 111:L041116, Jan 2025.
- [105] P. W. Anderson. Plasmons, gauge invariance, and mass. *Phys. Rev.*, 130:439–442, Apr 1963.
- [106] Peter W Higgs. Broken symmetries and the masses of gauge bosons. *Physical review letters*, 13(16):508, 1964.
- [107] G. Blatter, M. V. Feigel’man, V. B. Geshkenbein, A. I. Larkin, and V. M. Vinokur. Vortices in high-temperature superconductors. *Rev. Mod. Phys.*, 66:1125–1388, Oct 1994.
- [108] E H Brandt. The flux-line lattice in superconductors. *Reports on Progress in Physics*, 58(11):1465, nov 1995.
- [109] E. Zeldov, D. Majer, M. Konczykowski, V. B. Geshkenbein, V. M. Vinokur, and H. Shtrikman. hermodynamic observation of first-order vortex-lattice melting transition in $bi2sr2cacu2o8$. *Nature*, 375:373–376, 1995.
- [110] Alexander Altland and Ben D. Simons. *Condensed Matter Field Theory*. Cambridge University Press, 2010.
- [111] Konstantin Efetov. *Supersymmetry in Disorder and Chaos*. Cambridge University Press, 1999.
- [112] Alex Kamenev. Many-body theory of non-equilibrium systems, 2005.
- [113] Jürgen Fuchs and Christoph Schweigert. *Symmetries, Lie Algebras and Representations: A Graduate Course for Physicists*. Cambridge University Press, 2003.
- [114] Alexander Altland, Dmitry Bagrets, Lars Fritz, Alex Kamenev, and Hanno Schmiedt. Quantum Criticality of Quasi-One-Dimensional Topological Anderson Insulators. *Physical Review Letters*, 112(20):206602, 2014.
- [115] Alexander Altland, Dmitry Bagrets, and Alex Kamenev. Topology versus Anderson localization: Nonperturbative solutions in one dimension. *Physical Review B*, 91(8):085429, 2015.
- [116] John David Jackson. *classical Electrodynamics (Third Edition)*. Wiley, 1999.
- [117] V. N. Popov. Quantum vortices and phase transitions in bose systems. *Soviet Physics – JETP*, 37:341, 1973.
- [118] F.W. Wiegel. Vortex-ring model of bose condensation. *Physica*, 65(2):321–336, 1973.
- [119] Robert Savit. Vortices and the low-temperature structure

- of the $x - y$ model. *Phys. Rev. B*, 17:1340–1350, Feb 1978.
- [120] Michael E Peskin. Mandelstam-'t hooft duality in abelian lattice models. *Annals of Physics*, 113(1):122–152, 1978.
- [121] Eduardo Fradkin, B. A. Huberman, and Stephen H. Shenker. Gauge symmetries in random magnetic systems. *Phys. Rev. B*, 18:4789–4814, Nov 1978.
- [122] Ryuichi Shindou and Pengwei Zhao. Topological effect on order-disorder transitions in $u(1)$ sigma models. *Phys. Rev. B*, 111:224507, Jun 2025.
- [123] Akihiro Tanaka and Shintaro Takayoshi. A short guide to topological terms in the effective theories of condensed matter. *Science and Technology of Advanced Materials*, 16(1):014404, 2015.
- [124] Igor Herbut. *A Modern Approach to Critical Phenomena*. Cambridge University Press, 2007.
- [125] Michael Kiometzis, Hagen Kleinert, and Adriaan M. J. Schakel. Dual Description of the Superconducting Phase Transition. *Fortschritte der Physik*, 43:697–732, 1995.
- [126] Eduardo Fradkin. Critical behavior of disordered degenerate semiconductors. ii. spectrum and transport properties in mean-field theory. *Phys. Rev. B*, 33:3263–3268, Mar 1986.
- [127] Sergey V. Syzranov and Leo Radzihovsky. High-Dimensional Disorder-Driven Phenomena in Weyl Semimetals, Semiconductors, and Related Systems. *Annual Review of Condensed Matter Physics*, 9(1):35–58, 2018.
- [128] Nagaosa Naoto. *Quantum Field Theory in Condensed Matter Physics*. Springer-Verlag, 1999.